LA-UR-22-32917

Approved for public release; distribution is unlimited.

Title: Detonation Waves in High Explosives

Author(s): Menikoff, Ralph

Intended for: Lectures at LANL on high explosives

Issued: 2022-12-14

Los Alamos
NATIONAL LABORATORY

Detonation Waves in High Explosives

Ralph Menikoff, T-1

HE seminar series
November, 2022

Managed by Triad National Security, LLC for the U.S. Department of Energy's NNSA

Lectures: Detonation Waves in High Explosives

Lecture 1 outline

1. Introduction

What is an explosion

Conditions for an explosion

- Energetic material
  Can undergo an exothermic chemical reaction (release energy)
- Sufficiently high reaction rate and confinement
  To support a propagating reactive wave

Explosion is large energy release on short time scale

Examples

1. Catastrophic explosion of 2000 tons ammonium nitrate
   in Beirut, Lebanon (August 2020)
2. Aerosols: Suspensions of solid particles or liquid droplets in a gas
   - Fuel droplets in air
   - Coal dust in mine
   - Grain dust in silo
   - sugar particles in refinery, Port Wentworth, Ga (2008)

What is an explosive

Explosive

- Energetic material that contains both fuel and oxidizer
  In contrast, aerosol oxidizer from O_2 in air
  Particle surface burning requires diffusion of oxidizer
- Supports quasi-steady propagating reactive wave
  Called a detonation wave

Detonation wave

1. Lead shock triggers fast reaction
2. Reaction releases chemical energy
3. Energy release supports lead shock
4. Detonation wave can be self-sustaining (unsupported)

Once initiated a detonation wave is self-sustaining
and releases large amount of energy on μs time scale

Explosive applications

Applications of explosives

1. Mining, construction, demolition
2. Explosive welding, jet cutter with shaped charge, explosive bolts
3. Argon flash lamp, explosive art
4. Drive projectile to high velocity (several km/s)
   High pressure EOS data (LASL Shock Hugoniot Data, Ed. S. Marsh, 1980)
5. Explosive driven flux compression generator (30 MA at 10 kV)
6. Weapons

High explosives & Detonation waves

Compared to gaseous explosive, solid explosives have much higher density and higher energy per volume
They are referred to as high explosive (HE)

Solid high explosive with 1 reaction
Reactants $\rightarrow$ Products + energy release
Meta-stable reactants $\Rightarrow$ Irreversible reaction

Reactive burn models differ in

1. EOS used for partly reacted HE
2. Burn rate (not simply chemical rate)

Detonation wave (lead shock followed by reaction zone)

- For large burn rate $\sim$ 100 /μs and high detonation wave speed Reaction zone is very narrow, $\sim$ 0.1 mm
- Pressure rise is abrupt and shock 'like', especially for simulations with cell size comparable to the reaction zone width

Detonation wave properties

Detonation wave properties for PBX 9501

initial density	1.84	g/cc
pressure	35.	GPa
detonation speed	8.8	km/s
sound speed	6.6	km/s
energy release	5.0	MJ/kg

$C_4H_8N_8O_8 \rightarrow 4\,H_2O + 4\,N_2 + 4\,CO$

Perspective on energy release

sugar not explosive but burning $C_{12}H_{22}O_{11} + 12\,O_2 \rightarrow 12\,CO_2 + 11\,H_2O$
releases 3.94 kcal/g = 16.5 MJ/kg, more energy per mass than PBX 9501

Example

KE of 2 ton car at 100 mph = 1.8 MJ = 1 kWh
same energy as 5.8 cm cube (360 g) of PBX 9501 released in 6.6 μs

Also PBX 9501 can drive projectile up to sound speed (14.7×10^3 mph)

Detonation wave vs Shock wave

Both shock and detonation loci

- Hugoniot equation for 1-D waves
  $e = e_0 + \frac{1}{2}\big(P(V,e) + P_0\big)(V_0 - V)$
  P with reactants EOS for shock
  and products EOS for detonation
- Compressive waves
- Supersonic ahead
  Subsonic behind, CJ state sonic

click to zoom

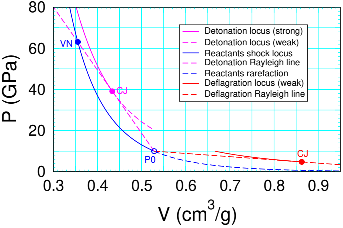

Detonation wave locus only

- Locus shifts up wrt initial state
- Rayleigh line tangent at ‘CJ’ point
- CJ (Chapman-Jouguet) state
  Minimum detonation speed
  Unsupported detonation & sonic
  Decouples from acoustic waves
- Above CJ state (strong branch)
  Overdriven detonation waves
  Decay without support, ‘shock like’
- Below CJ state (weak branch)
  Unphysical branch (no wave profile)
- Expansive deflagration branch
  Slow burn mode, low wave speed
  Explosive also propellant

Detonation wave width

Detonation wave reaction-zone width

return

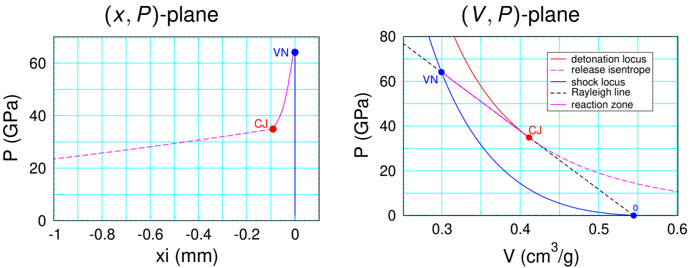

- Detonation profile

  From VN spike on reactants shock locus to CJ state on detonation loci
- In contrast to shock wave

  Detonation wave width is phyical length scale

  Depends on burn rate
- Effects detonation phenomena (*e.g.*, curvature effect)

Chemical energy released

Heat of detonation is change in enthalpy ($H = e + PV$) between products expanded out to $P = 0$ and reactants state

Heat release
$-\Delta$ enthalpy is area shown in red

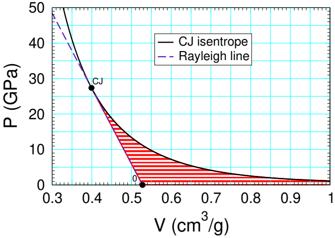

cylinder test

Cylinder test wall velocity

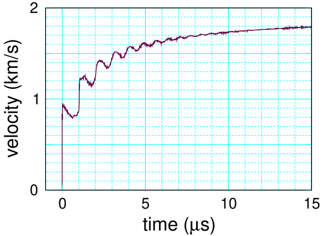

convert HE energy to KE of wall

Useful energy limited by expansion

At expansion of $V/V_0 = 7$, $P \approx 0.1$ GPa
and recover above 80 % of chemical energy

Measurement of energy released

- Bomb calorimeter
  Large volume implies small change in pressure when HE reacts
  1. Inert gas in calorimeter gives heat of detonation
  2. Air in calorimeter gives heat of combustion
     Additional reactions with oxygen in air
     For oxygen poor explosives, such as for TNT
- Heat of reaction
  Equilibrium products constituents mass fractions from thermo-chemical code
  (rapid expansion may freeze out products *e.g.*, liquid or gaseous H_2O)
  Reactants $\rightarrow \sum_i \nu_i \, \mathrm{prod}_i$ where ν_i are stoichiometry coefficients

$$\Delta H_{\mathrm{reaction}} = \sum_i \nu_i H_{\mathrm{prod}_i} - H_{\mathrm{reactants}}$$

  where H_{prod_i} and $H_{\mathrm{reactants}}$ are heats of formation
  and $\Delta H_{\mathrm{reaction}}$ is either heat of combustion or heat of detonation

Convention for heat release

$$Q = -\Delta H_{\text{reaction}} \begin{cases} > 0 & \text{for exothermic reaction} \\ < 0 & \text{for endothermic reaction} \end{cases}$$

End Lecture 1. Introduction

Questions

Lecture 2 outline

2. Solid high explosives
   - HE molecules
   - Plastic-bonded explosive
   - PBX manufacture
   - Example of meso-scale structure
   - Heterogeneities and burn rate
   - HE reactive burn models

HE molecules

TriNitro-Toluene

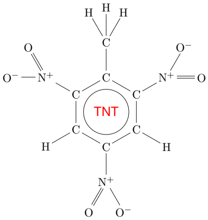

cyclo-tetramethylene-tetranitramine

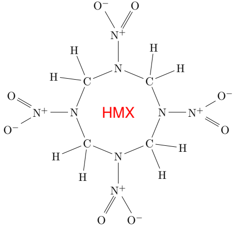

TriAmino-Trinitro-Benzene

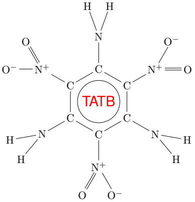

TNT (21 atoms): $C_7H_5N_3O_6 \rightarrow 2.5\,H_2O + 1.5\,N_2 + 3.5\,CO + 3.5\,C$

HMX (28 atoms): $C_4H_8N_8O_8 \rightarrow 4\,H_2O + 4\,N_2 + 4\,CO$

TATB (24 atoms): $C_6H_6N_6O_6 \rightarrow 3\,H_2O + 3\,N_2 + 3\,CO + 3\,C$

TNT melts at 80 C and thermal runaway at 228 C.

TNT can be cast or pressed into HE

HMX crystallites: coarse/fine similar size to table/powdered sugar

TATB crystallite slightly smaller than HMX

HMX or TATB crystallites need binder to form HE

Plastic-bonded explosive

Plastic-Bonded Explosive (PBX)

1. Explosive grains
2. Polymeric binder
3. pores

Examples

- PBX 9501, conventional HE (CHE)
  95 wt % HMX + 2.5 % estane + 2.5 % elasto-plasticizer
- PBX 9502, insensitive HE (IHE)
  95 wt % TATB + 5 % Kel-F

	TNT	HMX based PBX 9501	TATB based PBX 9502	
ρ_0	1.64	1.84	1.89	g/cc
P_{cj}	19.	35.	28.	GPa
D_{cj}	6.9	8.8	7.8	km/s
$-\Delta H_{det}$	4.2	5.0	3.5	MJ/kg

PBX manufacture

1. Batch of molding powder
   Combine coarse and fine HE grains
      Random closed packing of spheres, vol fraction 64 %
   Coat grains with binder to form granules (conglomerate of grains)
2. Blend batches into a lot
   Heterogeneities more similar within a lot than between lots
3. Heat and press molding powder to form PBX
   Compress out porosity to achieve specified density
      Grains can fracture and change size distribution
      Grain orientation can align with pressing direction

- PBX specification on molding powder
  Minimize local variations of heterogeneities
  Spatial average more uniform and behavior more reproducible
- Improve accuracy comparing experimental data
  Use same lot and correct for firing temperature and density

Example of meso-scale structure

click to zoom

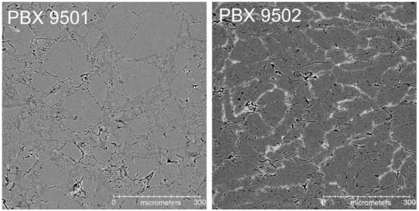

Computer X-ray micro-tomography images
Patterson *et al.*, 2020 fig 3a,b
Slices through samples (0.8 μm pixel size)
Can see grains and pores greater then 1μm
Issues with binder contrast and resolution
nano tomography of TATB grains
Patterson *et al.*, 2022
Smaller field of view with higher resolution

ultra-small angle neutron scattering (USANS)
Pore diameter ranged from 0.1 to 10 μm.
Analysis of volume averaged pore and binder size distributions depend on assumption for form factors (spherical, cylindrical)

- PBX 9501 Mang *et al.*, 2010
  Peak and mean pore diameter, 0.7 and 2.2 μm (spherical)
  Binder thickness peak and mean 0.14 and 0.16 μm (cylindrical)
- PBX 9502 Thompson *et al.*, 2010
  Large volume fraction of pores with diameter less than 1 μm

Heterogeneities and burn rate

Underlying physics issues

- Shock initiation experiments show
  Chemical reaction rate from shock temperature
  orders of magnitude too small for observed time to detonation
- Shock in heterogeneous HE
  Temperature variations behind lead shock
- Chemical rate temperature sensitive
  Localized regions of high temperature called ‘hotspots’
  Generated by pore collapse dominate burn rate
- Not feasible for simulations to resolve sub-micron hotspots
  Need sub-grid model for burn rate that averages out short wavelengths
    Burn rate is spatial average of chemical rate
    over length scale of heterogeneities

Burn rate depends on meso-scale structure of PBX

HE reactive burn models

Homogenized reactive burn model for heterogeneous solid HE

1. HE treated as homogeneous material
   Characterized by V, e and mass fraction of products λ
2. EOS for partly burned HE function of (V, e, λ)
   Typically, P, T equilibrium of reactants and products
3. Empirical burn rate to account for heterogeneities
   Distribution and dynamics of hotspots not understood (no data)
      well enough to develop sub-grid model for burn rate
   Typically burn rate strongly depends on P rather than T
      Major difference with gaseous detonation
4. Burn rate calibrated to experimental data
   Scatter in data from heterogeneities affects accuracy

Following lectures on theory then detonation phenomena
and experimental data that can be used to calibrate burn rate.

End Lecture 2. Solid high explosives

Questions

Lecture 3 outline

3. Reactive flow equations

   Model PDEs
   Single irreversible reaction
   EOS for partly burned HE
   P-T equilibrium
   Ideal explosive EOS
   Energy source term
   Characteristic equations
   Shock state & characteristics
   Shock acceleration

Model PDEs

Reactive Euler equations

Conservation form for one reaction progress variable λ

$$\partial_t \begin{pmatrix} \rho \\ \rho u \\ \rho(e + \frac{1}{2}u^2) \\ \rho\lambda \end{pmatrix} + \partial_x \begin{pmatrix} \rho u \\ \rho u^2 + \underline{P} \\ \rho u(e + \frac{1}{2}u^2 + \underline{P}V) \\ \rho u \lambda \end{pmatrix} = \begin{pmatrix} 0 \\ 0 \\ \rho Q \underline{\mathcal{R}} \\ \rho \underline{\mathcal{R}} \end{pmatrix}$$

ρ, u, e are density, particle velocity and specific internal energy

Q is specific energy release and $\mathcal{R}(V, e, \lambda)$ is reaction rate

Hydro and reaction coupled through the pressure $P(V, e, \lambda)$

For an explosive $\boxed{(\partial_\lambda P)_{V,e} > 0}$

Shock relations: mass and reaction equations imply λ is continuous

Last component reduces to rate equation (like ODE along particle path)

$$\boxed{(\mathrm{d}/\mathrm{d}t)\lambda = (\partial_t + u\partial_x)\lambda = \mathcal{R}}$$

Single irreversible reaction

Typical assumption on rate for solid HE

- λ is mass fraction of products
  Hence $0 \leq \lambda \leq 1$
- Irreversible reaction
  Hence $\mathcal{R} \geq 0$
- Rate vanishes when reactants depleted
  Hence, $\mathcal{R} \to 0$ as $\lambda \to 1$

- Why single reaction
  Homogenized burn model for heterogeneous solid HE
  Reactive wave outward from hotspots dominates burning
  Multi-step reactions on slower time scale of thermal ignition
- Why irreversible reaction
  Hotspot burn model implies fully burned reaction regions within background of reactants

EOS for partly burned HE

EOS: $P(V, e, \lambda)$, $T(V, e, \lambda)$

1. Reactants EOS for $\lambda = 0$, unreacted
2. Products EOS for $\lambda = 1$, completely burned
3. Mixture rule to interpolate for $0 < \lambda < 1$

Typically, P-T equilibrium for partly burned HE

- Gibbs free energy
  $G(P, T, \lambda) = \lambda G_p(P, T) + (1 - \lambda) G_r(P, T)$
  Unique solution provided reactants and products
  EOS are thermodynamically consistent and stable
- Products hotspots and reactants not in temperature equilibrium
  Calibrated rate can compensate for mixture rule
  Rate dominated by pressure (for most models)

In principle can use 2-phase model with 2 temperatures
Different set of issues (additional jump condition needed for energy)

P-T equilibrium

Frequently used mixture rule is *P*-*T* equilibrium

Given V, e, λ find V_p, e_p and V_r, e_r such that

$$P(V, e, \lambda) = P_p(V_p, e_p) = P_r(V_r, e_r)$$
$$T(V, e, \lambda) = T_p(V_p, e_p) = T_r(V_r, e_r)$$
$$V = \lambda V_p + (1 - \lambda) V_r$$
$$e = \lambda e_p + (1 - \lambda) e_r$$

Subscripts ‘p’ and ‘r’ denote products and reactants, respectively

Corresponds to phase separation between reactants and products

Evaluation of *P* and *T* requires iteration algorithm

Computationally more expensive than analytic EOS

Solid EOS in expansion may lose thermodynamic stability, $K_T < 0$ and P-T equilibrium solution break down

Ideal explosive EOS

Reactants (ideal gas)

$$P_r(V, e) = (\gamma - 1)e/V$$
$$T_r(V, e) = e/C_V$$

Products (ideal gas with energy offset Q)

$$P_p(V, e) = (\gamma - 1)(e + Q)/V$$
$$T_p(V, e) = (e + Q)/C_V$$

PT equilibrium

$$V_r = V_p = V$$
$$e_p = e - (1 - \lambda)\, Q$$
$$e_r = e + \lambda\, Q$$

Equivalent to

$$P(V, e, \lambda) = (\gamma - 1)(e + \lambda Q)/V$$
$$T(V, e, \lambda) = (e + \lambda Q)/C_V$$

Energy source term

Relative energy origins of products and reactants

PDEs invariant under transformation

$$P'_p(V, e) = P_p(V, e + q)$$
$$(\mathrm{d}/\mathrm{d}t)e = -P'(\mathrm{d}/\mathrm{d}t)V + (Q - q)(\mathrm{d}/\mathrm{d}t)\lambda$$

if EOS mixture rule satisfies $e = \lambda e_p + (1 - \lambda)e_r$

Heat release can be

- explicit, Q in energy equation
- or offset in energy origin between reactants and products q
- or both Hugoniot eq

Convention to eliminate energy source term

Chose $e_0 = 0$ for reactants and energy origin of products
such that $P_{cj} = P_p(V_{cj}, e_{cj})$ where $e_{cj} = \frac{1}{2}P_{cj} \cdot (V_0 - V_{cj})$
Then no source term in energy equation, *i.e.*, $Q - q = 0$

Characteristic equations

Acoustic wave families

return

$$(\mathrm{d}/\mathrm{d}t + c\partial_x)P + \rho c\,(\mathrm{d}/\mathrm{d}t + c\partial_x)u = s\mathcal{R}, \quad \text{along } \mathrm{d}x/\mathrm{d}t = u + c$$

$$(\mathrm{d}/\mathrm{d}t - c\partial_x)P - \rho c\,(\mathrm{d}/\mathrm{d}t - c\partial_x)u = s\mathcal{R}, \quad \mathrm{d}x/\mathrm{d}t = u - c$$

Contact wave families

$$(\mathrm{d}/\mathrm{d}t)P + (\rho c)^2(\mathrm{d}/\mathrm{d}t)V = s\mathcal{R}, \quad \text{along } \mathrm{d}x/\mathrm{d}t = u$$

$$(\mathrm{d}/\mathrm{d}t)\lambda = \mathcal{R}, \quad \mathrm{d}x/\mathrm{d}t = u$$

where

- $\mathrm{d}/\mathrm{d}t = \partial_t + u\partial_x$ is the convective time derivative
- S and T are entropy and temperature
- $s = (\partial_\lambda P)_{V,e} + \Gamma\rho Q$
- $\Gamma = (V\partial_e P)_{V,\lambda}$ is the Grüniesen coefficient

Characteristic velocities (wave speeds) are $u + c$, $u - c$ and u

Shock state & characteristics

Characteristics in rest frame of shock front

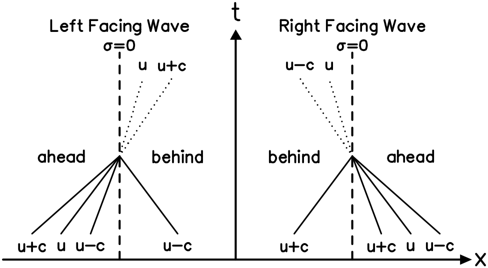

- Ahead state
  Determined by characteristics ahead of shock front
- Behind state
  Shock locus from ahead state
  Incoming characteristic behind front
  Source terms affect behind state

Shock acceleration

Pressure profiles at sequence of times

rarefaction wave
shock decays

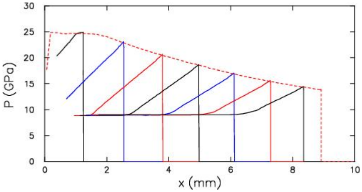

compressive wave
shock growths

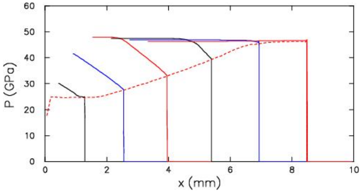

shock-to-detonation transition
reaction accelerates shock

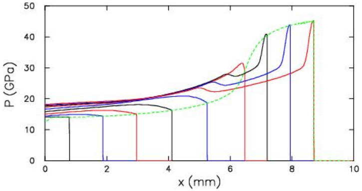

detonation wave

End Lecture 3. Reactive flow equations

Questions

Lecture 4 outline

4. Detonation wave relations

Shock relations

$$e = \lambda Q + e_0 + \frac{1}{2}\left[P(V, e, \lambda) + P_0\right] \cdot (V_0 - V)$$ ◂ return

$\lambda = 0$ gives reactants shock locus (reactants EOS)
$\lambda = 1$ gives the products detonation locus (products EOS)

- When ahead state is at rest $u_0 = 0$
  $P = P_0 + \rho_0 u D$ and $V/V_0 = 1 - u/D$
  Measurement of particle velocity and wave speeds u and D determines point on shock/detonation locus
- $\frac{P - P_0}{V_0 - V} = (\rho_0 D)^2$
  Slope of Rayleigh line in (V, P)–plane
- $(\Delta u)^2 = (P - P_0)(V_0 - V)$
  Change in particle velocity from thermodynamic variables

Straight forward to transform from (V, P)–plane to (u_p, D)–plane

CJ state relations

Jump relations and sonic condition imply ($P_0 = 0$)

$$P_{CJ} = \frac{\rho_0 D_{CJ}^2}{\gamma+1}$$

$$V_{CJ} = \frac{\gamma}{\gamma+1} V_0$$

$$u_{CJ} = \frac{D_{CJ}}{\gamma+1}$$

$$c_{CJ} = \frac{\gamma}{\gamma+1} D_{CJ}$$

where $\gamma = c^2/(PV)$ is adiabatic exponent at CJ state

- $D_{CJ} > c_{CJ} > \frac{1}{2} D_{CJ} > u_{CJ}$, if $\gamma > 1$
- Typically, for solid explosive $\gamma_{CJ} \approx 3$

Ideal HE EOS: $D_{CJ}^2 = 2(\gamma^2 - 1)Q$

- Detonation speed proportional to square root of Q
- Detonation pressure proportional to energy release Q

Shock and detonation loci

Example shock/detonation loci for PBX 9502

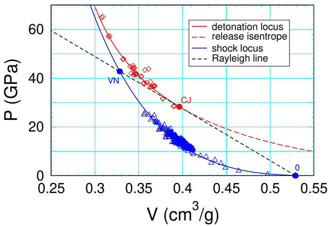

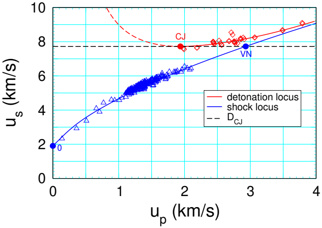

- Experiments measure u_p and u_s
  Determine P, V and e from shock relations
  Scatter in data partly from HE heterogeneities
- Overdriven detonation waves
  Experiments with flyer plate to support detonation
- Reactants shock Hugoniot
  Data limited by reaction, extrapolate to high P
  Constraint: Reactants and products loci do not cross if thermicity positive

Detonation speed dependence on initial state

- Density of PBX varies with porosity of pressing
  Detonation speed depends on energy release per volume
- Range of temperatures, $-55 < T < 75C$, for applications
  Thermal expansion affects initial density

Linearizing Hugoniot equation and sonic condition gives

$$\frac{\Delta D_{cj}}{D_{cj}} = A\,\frac{\Delta\rho_0}{\rho_0} + B\,\frac{\Delta e_0}{D_{cj}^2}$$

where

$$A = \frac{\gamma(\gamma - \Gamma - 1)}{2\gamma - \Gamma} \quad \text{and} \quad B = \frac{\Gamma}{2\gamma - \Gamma}\,(\gamma + 1)^2$$

γ is adiabatic exponent and Γ is Grüniesen coefficient

Typically, at CJ state $\gamma \approx 3$ and $\Gamma \approx 0.5$ would give $A \approx 0.82$ and $B \approx 1.45$

Ref: Fickett & Davis, Detonation (1979), §3B, “experimental test of theory”
Vary ρ_0 & T_0 for solid and liquid TNT, same equilibrium products return

Experimental reaction-zone profile

Profile experiments of Gustavsen *et al.*, 11th Detonation Symposium, 1998
VISAR velocity profiles of PBX 9501 detonation wave and simulations

PMMA window

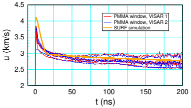

Li-F window

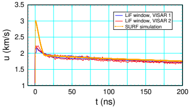

click fig to zoom/return

- VN spike is low
- Noise in signal
- Scatter in PMMA data

PDV velocity profiles (left) for 'PBX 9501 like' detonation wave into Li-F window and PDV signal spectrum (right) Pei *et al.*, 2019

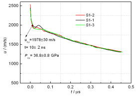

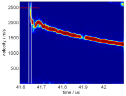

click fig to zoom/return

- large spread in spectrum at shock front

Polarized light micrographs for PBX 9501
Skidmore *et al.*, 11th Detonation Symposium, 1998, fig 4

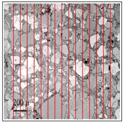

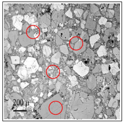

click fig to zoom/return

- Left fig red guide lines 100 μm apart about reaction-zone width
- Right fig red circles 200 μm diameter about spot size for VISAR and PDV

More details see LA-UR-20-24842 Menikoff, 2020 return

Detonation locus from EOS

- Point on detonation locus

  For fixed V, Newton iteration in e to solve

  $$e - e_0 - \tfrac{1}{2}(P_{prod}(V,e) + P_0)\cdot(V_0 - V) = 0$$

  Then jump relations to determine P_{cj} and u_{cj}
  Iteration converges rapidly since $(\partial_e P)_V = \Gamma(V,e)/V$ smooth function
  With Mie-Grüneisen type of EOS for products

  Γ function of only V and linear equation in e

- CJ state

  Parameterize detonation locus by V
  Bisection routine in V to find point on locus satisfying sonic condition

  $$\begin{aligned}(\rho c)^2 &= [\rho(D-u)]^2 = (\rho_0 D)^2 \\ &= (P - P_0)/(V_0 - V)\end{aligned}$$

  where V, $P(V)$ and $e(V)$ on detonation locus and $c_{prod}(V,e)$ from EOS
  Effectively, double iteration for CJ state

Programmed burn

Programmed burn model (Wilkins, 1964)

- Motivated by Chapman-Jouguet hypothesis
  Unique speed of unsupported detonation wave
  Applies to CHE with narrow reaction zone and small curvature effect
- Burn table for detonation time as function of position
  $t_{bt}(x)$ based on Huygens construction with constant wave speed D_{cj}
- Pseudo rate analogous to numerical dissipation for shock capturing

$$\mathcal{R}(x,t,\lambda) = \begin{cases} (1-\lambda)^n \tau^{-1} , & \text{if } t > t_{bt}(x) \text{ and } \lambda < 1; \\ 0 , & \text{otherwise;} \end{cases}$$

  where parameter τ is time constant and parameter $n < 1$
- Pseudo rate independent of hydro state
  No feedback to keep hydro front and burn front in sync
  Solution to PDEs may be unphysical
  In particular, if D for burn table not equal to D_{cj} from EOS

Solutions to PDEs for programmed burn model

- Burn table D greater than D_{cj} from EOS
  Reactive shock, detonation on weak branch of detonation locus

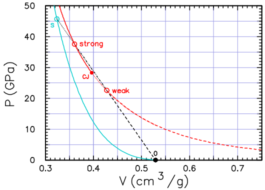

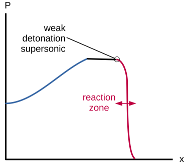

Unphysical for $D > D_{cj}$
- Reaction triggered arbitrarily
  Larger D gives smaller pressure
- Constant state behind detonation
  Head of rarefaction slower than detonation speed
- For $D = D_{cj}$ ok as approximation

- Burn table D less than D_{cj} from EOS
  Precursor shock followed by slower deflagration wave

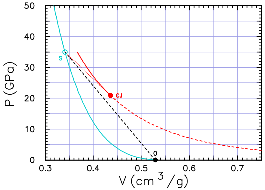

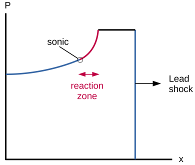

Unphysical for $D < D_{cj}$
- Split wave
  Shock followed by deflagration
- Burn out of sync with hydro front
  No feedback

End Lecture 4. Detonation wave relations

Questions

Lecture 5 outline

5. Planar detonation wave

Unsupported detonation wave

- Chapman-Jouguet detonation wave is shock like discontinuity propagating at the CJ detonation speed
  "Programmed burn" model for propagating detonation waves
- Zeldovich (1940), von Neumann (1942), Doering (1943)
  Modeled reaction zone due to finite rate (reactive fluid equations)
- Unsupported 1-D detonation
  Steady ZND reaction zone
  + Taylor wave (rarefaction) which spreads out in time
  End of reaction zone and head of rarefaction coincide

Wave diagram

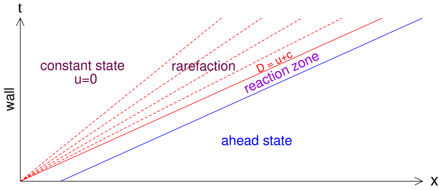

Wave profiles

Time sequence of pressure profiles for propagating detonation wave

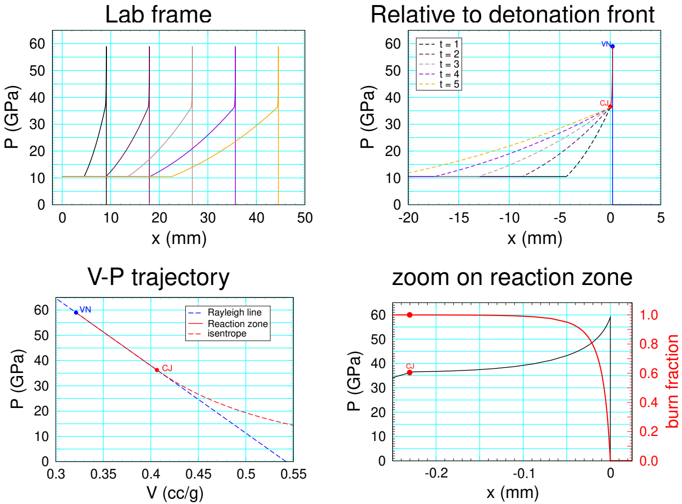

Reaction-zone width

Depletion factor: $\mathcal{R} \to 0$ as reactants burned up

$\mathcal{R} \propto (1-\lambda)^n$ as $\lambda \to 1$

Tail of wave profile

$(\mathrm{d}/\mathrm{d}t)\lambda = \mathcal{R}(\lambda)$

- $n < 1$

  Hotspot burn rate

  Finite burn time and reaction zone width

  $1-\lambda(t) \propto (t_* - t)^{1/(1-n)}$ as $t \to t_*$

  Important for curvature effect

- $n = 1$

  First order reaction

  exponential tail, $1-\lambda(t) \propto \exp(-t)$ as $t \to \infty$

- $n > 1$

  Reaction order for chemical reaction

  Algebraic tail, $1-\lambda(t) \propto t^{-1/(n-1)}$ as $t \to \infty$

Derivation of ZND profile

Partly burned detonation loci

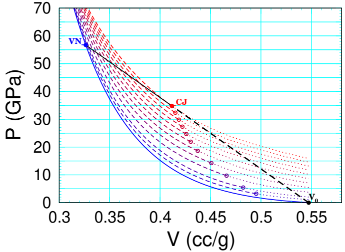

For details see LA-UR-22-29247 Menikoff, 2022

- For steady wave, $\xi = x - D\,t$ mass, momentum and energy fluxes are constant in rest frame of front
- In (V, P)–plane flow on intersection of Rayleigh line, slope $= -(\rho_0 D_{CJ})^2$ and partly burned detonation loci Parameterized points by λ ▸ Hugoniot eq

Rate equation reduces to ODE

$$(\mathrm{d}/\mathrm{d}\xi)\lambda = -\mathcal{R}\big(V(\lambda), e(\lambda), \lambda)\big)/[D - u(\lambda)]$$

where $V(\lambda)$, $e(\lambda)$, $u(\lambda)$ are point on partly detonation locus with detonation speed D, reduces to algebraic equation in 1 variable
Profile for strong branch of detonation locus, $D \geq D_{CJ}$

Detonation locus and Rayleigh line

Point of partly burned detonation locus with detonation speed D

Use jump condition to reduce to 1 equation for $V(\lambda)$

Newton iteration to find solution $f(V) = 0$

$$e_h(V) = \lambda Q + e_0 + \tfrac{1}{2} m^2 (V_0 - V)^2 + P_0\,(V_0 - V)$$

$$P_h(V) = P(V, e_h(V), \lambda)$$

$$f(V) = P_h - P_0 - m^2 (V_0 - V)$$

$$f'(V) = -(c/V)^2 + \Gamma\left[P_h - P_0 - m^2\,(V_0 - V)\right]/V + m^2$$

$$V \to V - f(V)/f'(V) \quad \text{Newton iteration}$$

where $m = \rho_0 D$ is mass flux for detonation speed
which defines Rayleigh line

For ODE for $\lambda(\xi)$ use last V to start iteration.

Algorithm very robust for any model EOS.

Taylor wave

1. ODEs for CJ isentrope of products EOS and velocity for rarefaction wave (right facing) ▸ characteristic equations

$$\frac{\mathrm{d}}{\mathrm{d}V}\begin{pmatrix} e \\ u \end{pmatrix} = -\begin{pmatrix} P(V,e) \\ c(V,e)/V \end{pmatrix}$$

   Integrate trajectory starting at CJ state $(V_{CJ},\ e_{CJ},\ u_{CJ})$
   til the back boundary condition is met (such as piston velocity)

2. Rarefaction wave (right facing)
   All variable (V, e, u) are constant on characteristics, $\mathrm{d}x/\mathrm{d}t = u + c$
   Characteristics are straight line in (t, x) ▸ wave diagram
   Characteristic speed is monotonic function of V
   for convex isentropes, $(\partial^2 P/\partial V^2)_S > 0$

Simulated PBX 9501 profile

- Numerical shock profile
  Rather than discontinuous shock
- Head of rarefaction/end of reaction zone
  Rapid but smooth transition
  Rather than kink
- With low resolution
  Burning in shock rise
  clip VN spike
- Release wave behind detonation
  Fairly insensitive to resolution

Planar propagating detonation wave
Verification test for reactive-hydro codes
Semi-analytic solution to compare with
For any EOS and any burn rate

High resolution simulation

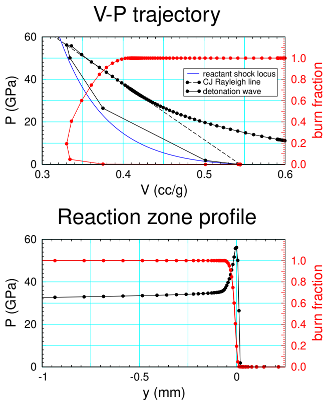

Compare Resolution

End Lecture 5. Planar detonation wave

Questions

Lecture 6 outline

6. Shock-to-detonation transition
   - Initiation mechanism
   - Shock initiation experiments
   - Pop plot data (ambient PBX 9502)
   - Pressure range for Pop plot
   - Temperature variation
   - Lot dependence
   - Density variation
   - Shock desensitization
   - Other shock initiation
   - HE initiation in a simulation

Initiation mechanism

Positive feedback mechanism for shock initiation

- Shock initiates reaction

  Hotspot burning for heterogeneous HE
- Reaction increase shock strength

  Source term in characteristic equation from reaction

  Pressure gradient forms due to reaction behind lead shock
- Increased shock pressure increases reaction rate

  More hotspots and increased burning around each hotspot

Shock-to-detonation transition

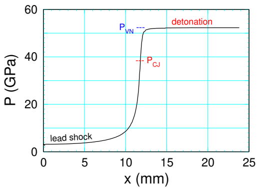

$P_s(x)$ similar to $T(t)$ for “cook-off” experiment

induction regime then runaway regime

run distance not sensitive to transition criterion

Shock initiation experiments

1-D shock initiation with sustained shock

- Wedge experiment (1960s)

  Lead shock trajectory
  Shock breakout on wedge
  Outruns side rarefaction
  Phase velocity $u_s / \sin(\theta) > c$
  Booster/Attenuator minimizes pressure gradient

- Gas gun experiment (late 1990s)

  Embedded magnetic velocity gauges
  25 μm Teflon + 5 μm Al + 25 μm Teflon

  Tracker gauge for shock trajectory
  Lagrangian velocity time histories
  Vary shock loading with material layers on projectile
  e.g., double shock, short shock

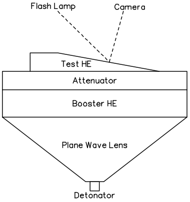

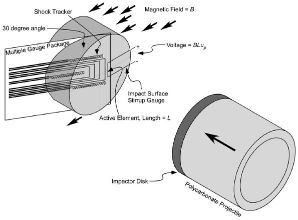

Gustavsen *et al.*, (2006), fig 1

Pop plot data (ambient PBX 9502)

Example data for each experiment

shock trajectory

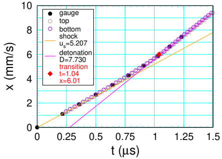

velocity profiles

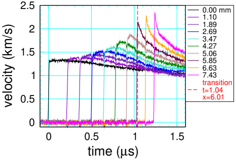

Pop plots, each point separate experiment

distance-of-run

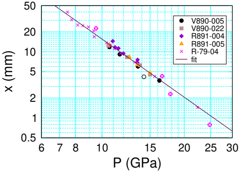

time to detonation

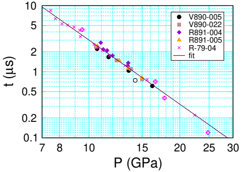

$x(t)$

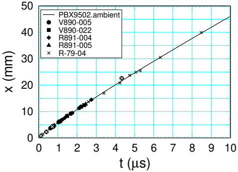

Pop plot: fits linear on log-log scale (empirical relation)

Power law dependence

Both run distance and run time, hence $x(t)$

Pressure range for Pop plot

Limitations on Pop plot data

- Low pressure
  Large run distance
  Sustained drive pressure limited by side rarefactions
  Pore collapse not effective at low pressures
    PBX shock width due to visco-elastic and elastic-plastic effects
    Run distance greater than linear fit on log-log plot
  Data for HMX based PBXs (projectile from 6 inch howitzer) show
    Run distance and run time bend upward at low pressures

  HMX Pop plot

- High pressure
  Short run distance
  Large uncertainties in shock trajectory and initial shock pressure
  Near P_{cj} or run distance $\sim$ steady reaction-zone width
    Approach to steady wave rather than initiation

Temperature variation

PBX 9502, T = 77 K, -55 C, 23 C, 76 C, 130 C

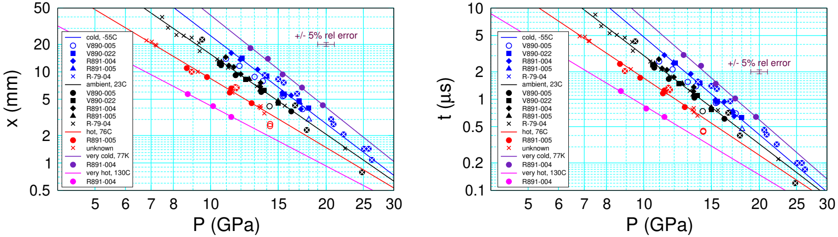

See Menikoff (2019) for references to experiments

- Shock sensitivity
  More sensitive explosive has shorter run distance
- As temperature increases
  More sensitive
- Scatter in data ($\pm 7\,\%$ for fixed P & outliers up to $30\,\%$)
  Uncertainties from experiment
  Sample variation from heterogeneities

Lot dependence

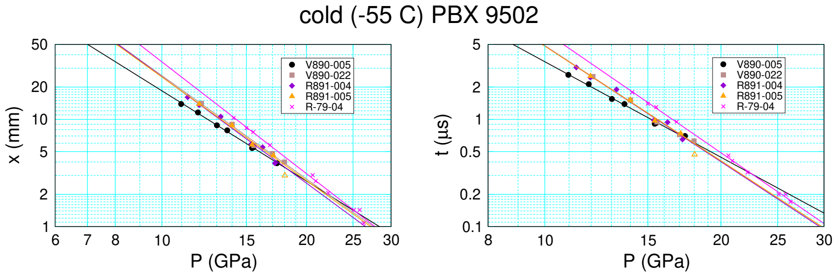

- Large lot dependence
  Greater than uncertainty in data
  Correlated variation in run time and run distance
- Burn rate affected by variation in heterogeneities
  Model parameters need to be fit for each lot
  or loss accuracy and potentially predictivity
- Issue for detonator/booster systems

Density variation

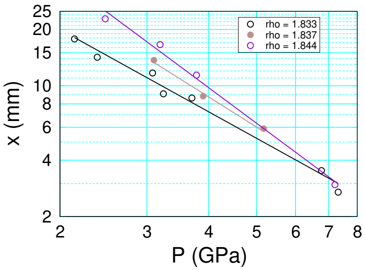

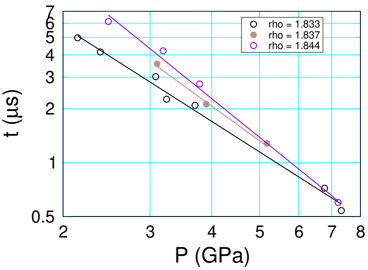

Gustavsen *et al.*, 1999, fig 12

- PBX 9501 pressing density
  1.833, 1.837 and 1.844 g/cc
  small density variation ± 5 mg/cc or ± 0.3 %
  large change in porosity ± 20 %
- Run distance at 3 GPa, 11 to 19 mm or ± 25 %
- Run time at 3 GPa, 3 to 4.5 μs or ± 20 %

Shock desensitization

Double shock PBX 9502

shot	P1 GPa	P2 GPa
2s450	5.3	19
2s463	7.0	25
2s465	9.0	33

VISAR data

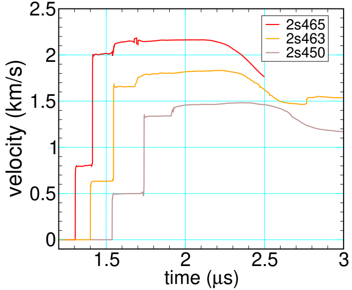

- Double shock
  Rate set by first shock
- Single crystal HMX very insensitive compared to PBX 9051
  Failed to detonate in 7 mm at shock pressure of 34 GPa
- Interpretation
  First shock closes pores and sets hotspot density
- Rate behind second shock
  About same as rate behind first shock

Other shock initiation

Complex shock loading

- Short shock

  Time duration of shock less than time to detonation

  Layered gas gun projectile high/low impedance

  Transverse wave from fragment impact

- Multiple shocks

  Shock desensitization

  Layered gas gun projectile low/high impedance

  Weak transverse shock can quench propagating detonation wave

  Dead zones for corner turning

- Shock followed by rarefaction

  Gap test

  Detonation wave in donor HE → inert → acceptor HE

- Shock initiation with divergent lead shock

  Detonator / booster

HE initiation for simulation

Initiate detonation wave in simulation

- Macroscopic 'hotspot'
  Small region of high pressure in simulation
  For example products at CJ state
- Drives shock into reactants
  Riemann problem, hotspot $\rightarrow$ reactants
  Determines lead shock pressure
- Prompt shock-to-detonation transition
  Hotspot needs to maintain pressure
  for time to detonation on Pop plot
  at reactants shock pressure
  Similar to 1-D short shock initiation

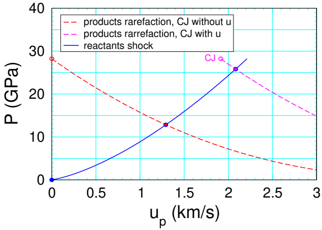

Hotspot plays role of a detonator/booster
Or programmed burn HE to generate hotspot

End Lecture 6. Shock-to-detonation transition

Questions

Lecture 7 outline

7. Hotspot burn rate
   - Properties of initiation data
   - Chemical rate
   - Homogeneous vs Heterogeneous initiation
   - Quench propagating detonation wave
   - Ignition & Growth concept
   - Hotspot requirements
   - Pore collapse as hotspot mechanism for shock initiation

Properties of initiation data

Motivation for hotspot burn rate

1. Rate much larger than chemical rate at shock temperature

   next slide

2. Homogeneous and heterogeneous shock initiation

   Qualitative different velocity profiles

   second next slide

3. Shock desensitization

   Double shock initiation data

   Single crystal HMX insensitive compared to PBX 9501
   previous lecture

   Quenching of propagating detonation wave

   third next slide

4. Run distance-to-detonation

   Sensitive to porosity

   previous lecture

Chemical rate

Reactants shock temperature

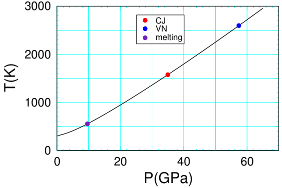

- 3 GPa on Pop plot for PBX 9501

  Time to detonation 4 μs
- Shock temperature 358 K
- Melt temperature, 550 K

  Thermal initiation time, $\sim$ 5000 s
- Chemical rate at shock temperature

  Orders of magnitude too low

Hotspots reconcile discrepancy

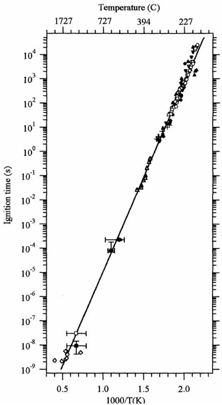

Henson-Smilowitz (2002), fig 1

PBX 9501 global rate

Homogeneous vs Heterogeneous initiation

Chemical rate at bulk temperature vs hotspot rate

Campbell *et al.*, (1961) homogeneous ignition and heterogenous ignition

- Homogeneous shock initiation
  Thermal runaway near HE interface
  Leading to super-detonation wave
  in shock compressed HE Detonation
  overtakes lead shock
- Heterogeneous shock initiation
  Reaction behind lead shock
  Shock strengthens to detonation
- Adding glass beads to nitromethane
  Velocity profiles change character
  from homogeneous to heterogeneous
  Also bubbles in liquid nitroglycerin

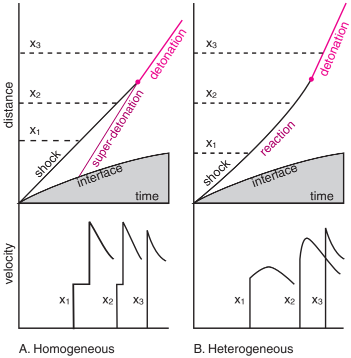

Quench propagating detonation wave

Detonation wave
in PBX 9502

Transverse shock
from steel flyer plate

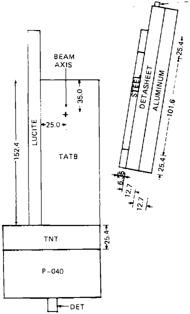

Phermex shot # 1697

static dynamic

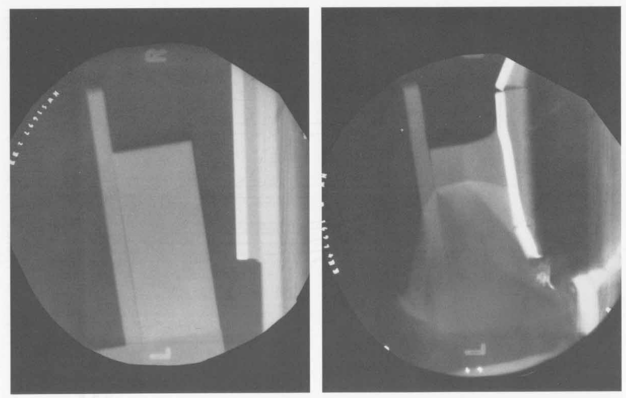

Ignition & Growth concept

Hotspots for initiation by friction and impact (Bowden & Yoffe, 1952)
Hotspots for shock initiation in heterogeneous HE (Campbell *et al.*, 1961)

Ignition & Growth concept (Lee & Tarver, 1980)

- Shock front triggers hotspots
  Pore collapse on fast time scale
- Burn centers
  Competition: heat conduction & reaction
  - Small hotspots quench
  - Large hotspots become burn centers
- Reactive wavelets
  Deflagration wave from burn centers
  Burn rate = (front area) · (deflagration speed)
- Depletion of reactants
  Overlap of reactive wavelets
  Geometric effect on front area

Potential hotspot sites

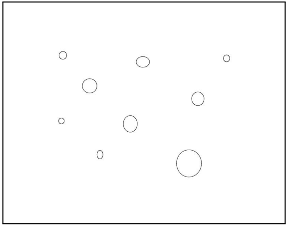

Pores or cracks
inter- or intra-granular

Ignition & Growth concept – pore collapse

Ignition & Growth concept (Lee & Tarver, 1980)

- Shock front triggers hotspots
  Pore collapse on fast time scale
- Burn centers
  Competition: heat conduction & reaction
  - Small hotspots quench
  - Large hotspots become burn centers
- Reactive wavelets
  Deflagration wave from burn centers
  Burn rate = (front area) · (deflagration speed)
- Depletion of reactants
  Overlap of reactive wavelets
  Geometric effect on front area

Shock sweeps over pores

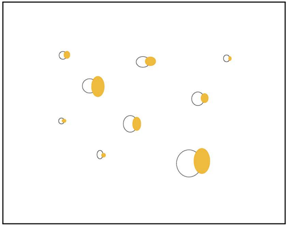

Hotspots form

Localized spatial regions of high temperature

Ignition & Growth concept – Ignition phase

Ignition & Growth concept (Lee & Tarver, 1980)

- Shock front triggers hotspots
  Pore collapse on fast time scale
- Burn centers
  Competition: heat conduction & reaction
  - Small hotspots quench
  - Large hotspots become burn centers
- Reactive wavelets
  Deflagration wave from burn centers
  Burn rate = (front area) · (deflagration speed)
- Depletion of reactants
  Overlap of reactive wavelets
  Geometric effect on front area

Ignition phase

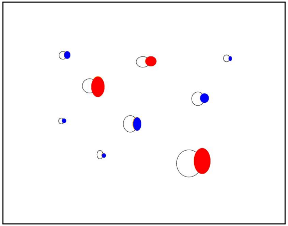

Hotspots react
some form burn centers

average $\mathcal{R}(T) \gg \mathcal{R}(\text{average } T)$

Burning dominated by
tail of temperature distribution

Ignition & Growth concept – early growth phase

Ignition & Growth concept (Lee & Tarver, 1980)

- Shock front triggers hotspots
  Pore collapse on fast time scale
- Burn centers
  Competition: heat conduction & reaction
  - Small hotspots quench
  - Large hotspots become burn centers
- Reactive wavelets
  Deflagration wave from burn centers
  Burn rate = (front area) · (deflagration speed)
- Depletion of reactants
  Overlap of reactive wavelets
  Geometric effect on front area

Early growth phase

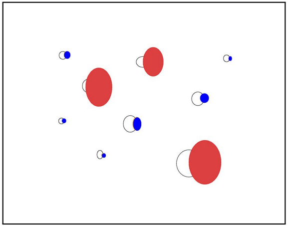

Burn front area increases

Reactants & products
are phase separated

Ignition & Growth concept – late growth phase

Ignition & Growth concept (Lee & Tarver, 1980)

- Shock front triggers hotspots
  Pore collapse on fast time scale
- Burn centers
  Competition: heat conduction & reaction
    Small hotspots quench
    Large hotspots become burn centers
- Reactive wavelets
  Deflagration wave from burn centers
  Burn rate = (front area) · (deflagration speed)
- Depletion of reactants
  Overlap of reactive wavelets
  Geometric effect on front area

Late growth phase

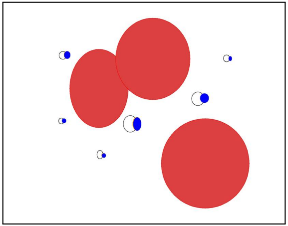

Depletion limited

Burn front area decreases

Hotspot requirements

- Minimum hotspot temperature
  Pop plot run time to detonation for PBX 9501: 4 μs at 3 GPa
  Hotspot thermal ignition time much shorter than run time ▸ gauge
  (little reaction in ignition phase, volume of hotspots is small)
  Estimate based on Henson-Smilowitz global rate for HMX (PBX 9501)
    Temperature greater than 1100 K at 3 GPa ▸ rate
  Need dissipative mechanism to localize energy in hotspot
- Hotspot size range
    (deflagration wave width) $<$ (hotspot size) $<$ (detonation wave width)
  Estimated hotspot size between 0.1 μm and 5 μm
    USANS data goes to smaller sizes
    Manufacturing defect if pores on the order of small grain size
  Single hotspot can trigger deflagration but not detonation
- Number density of pores
  For fixed porosity, number density scales as (pore size)$^{-3}$

Pore collapse as hotspot mechanism for shock initiation

Pore collapse properties

- Produces sufficiently high temperatures for hotspots
  Either shock heating from micro-jetting or viscous heating
- Peak temperature increases with shock pressure
  More burn centers and faster rate at higher shock pressure
- Consistent with shock sensitivity
  More pores at higher porosity and faster rate
- Consistent with shock desensitization
  First shock crushes pores and eliminates potential hotspot sites
- Consistent with low pressure Pop plot data
  Linear Pop plot (log-log scale) breaks down at low pressure

In the pressure range of Pop plot data
other mechanism don't produce sufficient heating

Below pressure of Pop plot data other mechanism needed
Such as shear heating for low velocity impact

End Lecture 7. Hotspot burn rate

Questions

Lecture 8 outline

8. Diameter effect and curvature effect

Unconfined rate stick experiment

- Cylinder of HE surrounded by air return
  Initiate at one end and run long enough to reach steady state
  rule of thumb, length 4 times the diameter
- Measurements
  Timing pins for axial detonation speed
  Curvature effect: Wave breakout along diameter with streak camera

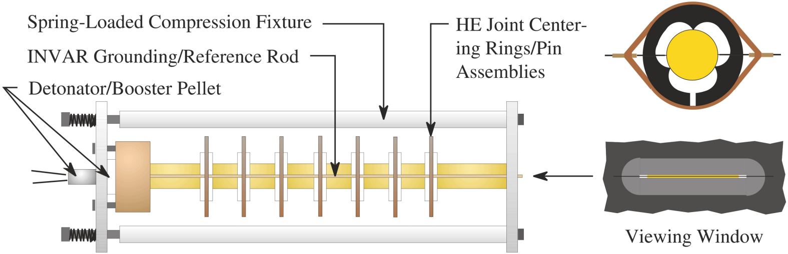

Hill *et al.*, 11th Detonation Symposium (1998)

Diameter effect

- Axial detonation speed for unconfined rate stick diameters
  Detonation speed decreases as diameter decreases
  Less than D_{CJ}, minimum based on shock jump conditions
- Minimum (failure) diameter to propagate detonation wave
- Limit of large diameter, $D_z(R)/D_{CJ} \to 1 - a/R$ as $R \to \infty$

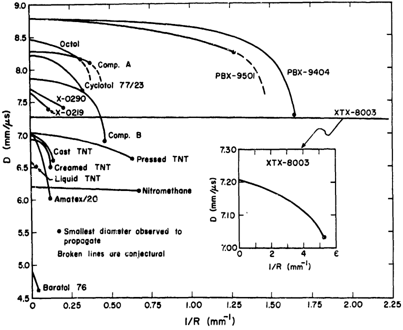

Detonation speed vs 1/R
Campbell & Engelke (1976)
6th Detonation Symposium

Modified jump conditions

- Stream tube in rest frame of detonation front

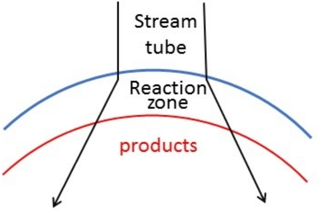

Blue is lead shock front
Red is end of reaction zone
subscripts 'a' and 'b' denote states ahead and behind reaction zone
'A' is cross sectional area
Diverging wave front if $A_b > A_a$

Duct flow equations

Flux is proportion to cross sectional area

At shock front $\mathrm{d}\ln(area)/\mathrm{d}x = \kappa$, sum of principal curvatures

- Partly burned detonation loci

Correction to jump conditions from reaction-zone width + front curvature

Diverging detonation wave, $\kappa > 0$

Sonic point lies within reaction zone

Detonation speed decreases with front curvature κ

1-D duct flow equations & jump conditions

$$\partial_t \begin{pmatrix} \rho A \\ \rho A u \\ \rho A(e + \frac{1}{2}u^2) \\ \rho A \lambda \end{pmatrix} + \partial_x \begin{pmatrix} \rho A u \\ \rho A u^2 + AP \\ \rho A u(e + \frac{1}{2}u^2 + PV) \\ \rho A u \lambda \end{pmatrix} = \begin{pmatrix} 0 \\ P\partial_x A \\ -P\partial_t A + \rho A Q \mathcal{R} \\ \rho A \mathcal{R} \end{pmatrix}$$

For quasi-steady detonation: $\mathrm{d}\ln(A)/\mathrm{d}x = \kappa$ is constant and $\partial_t A = 0$
Re-express PDEs in conservation form with additional geometric source term

$$\partial_t \begin{pmatrix} \rho \\ \rho u \\ \rho(e + \frac{1}{2}u^2) \end{pmatrix} + \partial_x \begin{pmatrix} \rho u \\ \rho u^2 + P \\ \rho u(e + \frac{1}{2}u^2 + PV) \end{pmatrix} = \begin{pmatrix} 0 \\ 0 \\ \rho Q \mathcal{R} \end{pmatrix} - \kappa \begin{pmatrix} \rho u \\ \rho u^2 \\ \rho u(e + \frac{1}{2}u^2 + PV) \end{pmatrix}$$

and $(\mathrm{d}/\mathrm{d}t)\lambda = \mathcal{R}$

For partly burned detonation loci, steady wave variables function of $\xi = x - Dt$
Integrating across reaction zone, no longer perfect differential
Jump conditions no longer algebraic expressions depend on rate as well as EOS

$$\kappa = \begin{cases} 1/x & \text{PDEs corresponds to cylindrical-symmetric flow; } x = r\text{, independent of } z \text{ \& } \theta \\ 2/x & \text{PDEs corresponds to spherically-symmetric flow; } x = r\text{, independent of } \theta \text{ \& } \phi \end{cases}$$

Characteristic equation

Extra geometric source term for diverging wave

For right facing characteristic, $\mathrm{d}x/\mathrm{d}t = u + c$

$$(\mathrm{d}/\mathrm{d}t + c\partial_x)P + \rho c(\mathrm{d}/\mathrm{d}t + c\partial_x)u = \left[\Gamma\rho Q + (\partial_\lambda P)_{V,e}\right]\mathcal{R} - \kappa\rho c^2 u$$

Shock-to-detonation transition is competition among

1. Pressure gradient behind shock front
2. Chemical reaction
3. Geometric source term for divergent flow

Curvature effect

- Theory, Bdzil, Stewart, Aslam (circa 1990)
  To first order in $\kappa \cdot$ (reaction-zone width)
  Can neglect transverse flow in duct and curvature of streamlines
  Duct flow PDEs reduce to ODEs for quasi-steady wave
  ODEs determine reaction-zone profile ▸ profile ODEs
  and for unsupported detonation waves the curature effect, $D_n(\kappa)$
  Detonation speed normal to front as a function of front curvature
- Reaction-zone width is important length scale
  Slope of $D_n(\kappa)$ strongly depends on reaction-zone width
  Hence burn rate at high pressure, $P_{cj} \lesssim P \lesssim P_{vn}$
  Numerical resolution affects detonation speed ▸ examples
- Diameter effect vs Curvature effect
  Diameter effect, D_z vs $1/R$, is global for unconfined rate stick
  Curvature effect, $D_n(\kappa)$ is local, material property
  It can predict diameter effect

Detonation Shock Dynamics (DSD)

DSD theory developed by Bdzil, Stewart, Aslam (circa 1990)

Reaction zone to sonic point decouples from flow behind

- Boundary condition
  From angle with inert determined by shock polar analysis ▸ shock polar
  Most important, sonic point on shock polar for weak confinement
- Time evolution of detonation front
  $D_n(\kappa)$ + boundary angle determines evolution of front using level set algorithm
  Precompute burn time table, $t_{bt}(\vec{x})$, before hydro simulation
- Model for propagating diverging detonation wave
  Generalization of programmed burn model
  front curvature dependent wave speed
- State behind detonation front
  Depends on numerical reaction-zone width
  Issue for simulations with coarse resolution

Converging or overdriven detonation wave

- Cylindrical or spherically converging shock wave
  Guderley similarity solution for polytropic EOS
  Shock velocity hence shock pressure increases as shock propagates
- Converging detonation wave
  Detonation speed increases as detonation propagates
- Overdriven detonation wave
  Collision of diverging fronts ▸ example
  Interaction portion of front is overdriven

In either case

- Reaction zone is subsonic (with respect to) front
  Analog of planar overdriven detonation wave
  Supported by flow behind reaction zone
- DSD assumption breaks down
  Detonation wave does not decouple from flow behind

Experimental measurement of $D_n(\kappa)$

Unconfined rate stick experiment

rate stick

- Axial detonation speed, D_z
  Determined from timing pins
- Front shape, $z(r)$
  Determined from streak camera breakout time along diameter
  Detonation front, 2-D surface of revolution about cylinder axis
- Front curvature, κ
  Fit front shape $z(r)$ with analytic function
  From first and second derivative calculate κ
  Principal components of curvature tensor
  radial and azimuthal directions
- Normal detonation speed, D_n
  $D_n = cos(\theta) \cdot D_z$ where $\tan(\theta) = dz/dr$
- $D_n(\kappa)$ determined parametrically
  D_n and κ as functions of r

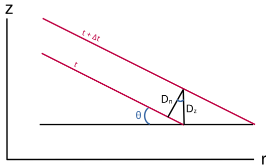

Example curvature effect

Normalized curvature effect for PBX 9501 and PBX 9502

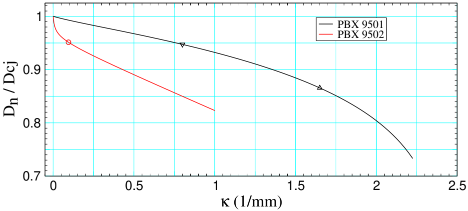

diameter effect

- $D_n(\kappa)$ for PBX 9501 representative of CHE
  Small initial slope $dD_n/d\kappa$ due to large burn rate (narrow reaction-zone width)
- Shape of $D_n(\kappa)$ curve for PBX 9502 PBX 9502 profile
  PBX 9502 has fast (hotspot) and slow (carbon clustering) burn rates
  Large variation in reaction-zone width for small κ
  sonic point shifts from end of slow reaction to near end of fast reaction
  Large slope $dD_n/d\kappa$ for small κ and then smaller slope due to fast reaction

End Lecture 8. Diameter effect and curvature effect

Questions

Lecture 9 outline

9. Failure diameter, corner turning and dead zones

Breakdown of DSD assumptions

DSD assumes $D_n(\kappa)$ independent of geometry

- PBX 9502 experiments show $D_n(\kappa)$ depends on diameter of rate stick
- Lead shock pressure changes rapidly in boundary layer
  Related to failure diameter & sonic boundary condition
- Transverse gradients not accounted for in duct flow PDEs (1-D)
  Profile ODEs may not have solution for large κ
  Nevertheless, 2-D simulations can fit shape of detonation front

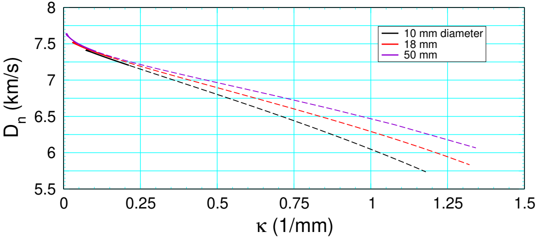

Hill, Bdzil & Aslam, 11th Detonation Symposium (1998)

Boundary layer

normalized front shape

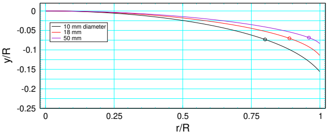

curvature vs normalized radius

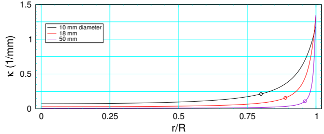

$P_s(r)$ within 5 mm of boundary

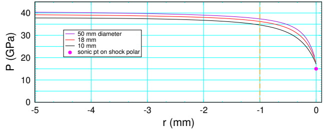

- Front shape $y(r)$ from experiment
  Flatter than it looks, aspect ratio 2 : 1
- Curvature κ from front shape
  up to 1.4/mm at boundary
  but $<$ 0.25/mm up to 1 mm of boundary
- Shock pressure
  Calculated from D_n and reactants shock locus
  Shock locus from assumed EOS
- Boundary pressure
  Sonic pressure from D_y and shock polar
  About 1/2 pressure on axis
  Large ΔP_s between axis and boundary
- Boundary layer
  Pressure gradient dP_s/dr
    small up to 1 mm of boundary
    large within 1 mm of boundary

Transverse energy flux

PBX 9502 failure diameter of 8.5 to 9 mm

Simulation of 10 mm diameter unconfined rate stick

streamlines and sonic locus

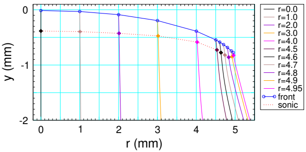

radial energy transfer

$d\rho E/dt$ along shock front

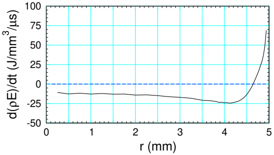

- Detonation wave profile ODEs apply along streamlines
  Sonic locus intersects shock front at boundary
- Detonation
  Supported by energy release along between front and sonic point
  Not sufficient for neighborhood of boundary
- Neighborhood of boundary
  Radial pressure gradient leads to radial energy flux
  Lead shock supported by energy flux from interior

Rate stick simulation near failure

Start with detonation wave in large diameter cylinder
Initiates slightly overdriven detonation in small diameter cylinder

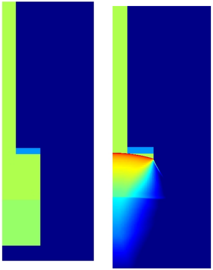

Two cases for PBX 9502
1. 10 mm diameter, above failure diameter
2. 8 mm diameter, below failure diameter

Failure mechanism

- Transverse energy flow behind front
  Weak lead shock in boundary layer
  Very low burn rate behind weak shock
- Failure wave
  Transverse radial flow in reaction zone
  drains energy from detonation
  Detonation front shrinks in radial extent
  Larger energy drain on detonation
- Weak shock after failure

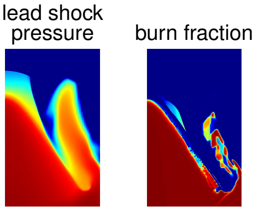

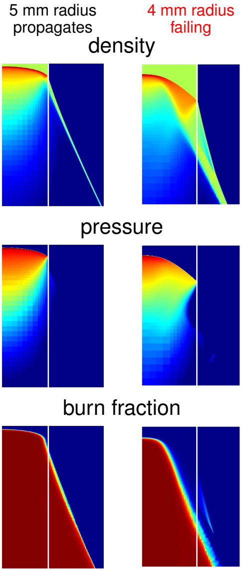

Additional comments on failure

Detonation wave failure

- Depends on geometry
  Unconfined rectangular slab of HE
  failure thickness $<$ failure diameter
- Depends on confinement
  Strong confinement, such as by steel
  Shock polar analysis at boundary
    Lead HE shock is subsonic ▸ shock polar
    Higher boundary pressure and smaller failure diameter
    Issue with boundary layer reduced or eliminated
  Caveat: To apply shock polar analysis at boundary
    No gap between HE and confiner
      For example, assembly tolerance in cylinder test ▸ cylinder test
    Otherwise sonic condition at boundary
    Weak confinement (filler or glue) also sonic condition
      Same front shape and detonation speed

PBX 9501 failure diameter

diameter effect

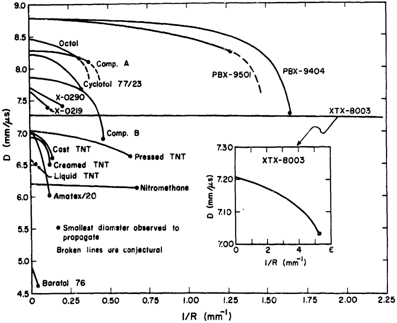

mesoscale structure

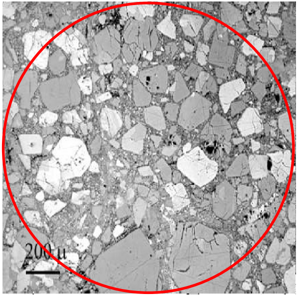

←——— 1.8 mm ———→

For rate stick near failure diameter (≈ 1.8 mm for PBX 9501)

Expect statistical variations of HE grain distribution on mesoscale
to cause fluctuations from localized failure and reignition along boundary
similar to what is seen for gaseous or liquid detonation due to instabilities that cause transverse waves

Corner turning – experiment

setup

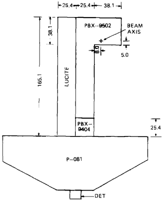

Shot 1941

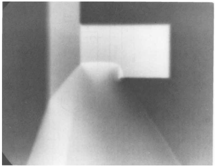

Shot 1796

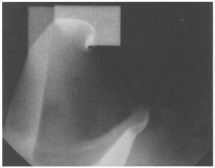

Shot 1943

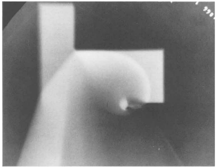

Phermex shots (1975, 1976)

- Time evolution
  Three experiments with 1 radiograph per shot
  Diffraction of lead shock lowers pressure
  Detonation spreads out laterally
- Dead zone
  Region of low rate or shock desensitized

Corner turning – simulation

- Setup similar to experiment

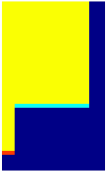

- Small HE cylinder width
  Affects corner turning
  and extent of dead zone
- Applications
  Detonator-booster
  Fragment impact
- Programmed burn or DSD
  Not intended for either
  ignition or dead zones

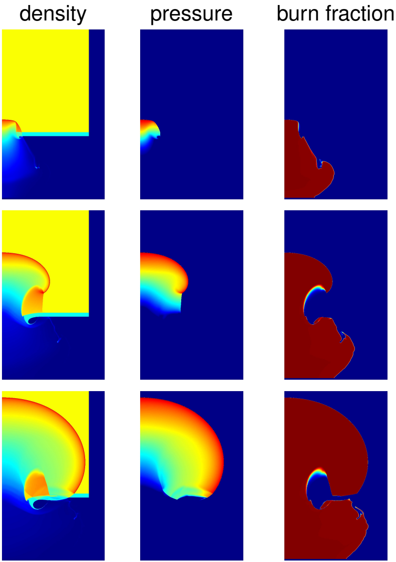

End Lecture 9. Failure diameter, corner turning and dead zones

Questions

Lecture 10 outline

10. EOS data

Needed PBX data

Before calibrating burn rate

- Reactants EOS data

  Prefer EOS for theoretical maximum data (TMD), no porosity

  Porosity model for initial PBX density

  porosity $= 1 - \rho_0/\rho_{TMD}$ determines initial density

  Reactants EOS independent of initial PBX state

  Reactants EOS should be consistent with P_s for Pop plot data

  P_s from impedance match from projectile into PBX

- Products EOS data

  Energy offset consistent with convention previously stated

  Offset convention only at 1 initial density

  Equilibrium products EOS independent of initial PBX state

  Reaction-zone fluctuations affect homogenized products EOS ?

- CJ state

  Detonation speed and pressure

Fickett & Davis

Reactants EOS

Available data to calibrate EOS model

- Principal shock Hugoniot
  Limited pressure range due to reaction
  Possibly take advantage of shock desensitization
  Reverse impact experiments
- Diamond anvil cell for isothermal compression
  Powder diffraction on small HE crystals not PBX
  Density measurement not accurate at high pressures
- Specific heat from phonon frequencies (measured or DFT)
  C_V varies by factor of 2 between ambient and VN spike
  Shock temperature measurements based on Raman scattering
- Molecular dynamics simulations
  Force fields available for HMX, RDX, TATB
  Mixture for HE crystallites plus binder

Products EOS data

Minimum data needed for good model

- CJ state
  - Detonation speed & pressure
- Overdriven detonation locus
  - Requires supported planar wave
- CJ release isentrope
  - 1-D release isentrope from overdriven detonation
    - Grüneisen coefficient from pair of overdriven isentropes
    - Γ allows extrapolating in e off the release isentrope
  - 2-D Cylinder test or Sandwich test or Disc Acceleration Experiment (DAX)
    - Unlike shock Hugoniot, infer isentrope with simulations for fitting form

Alternative, thermo-chemical code

BKW (Mader), CHEETAH (LLNL), MAGPIE (PEM-LANL)

Calculate equilibrium species, then uses P–T equilibrium

Typically, needs to be tweaked for greater accuracy

Cylinder test experiment

- Standard test
  1 inch diameter HE
  0.1 inch thick copper tube
  2 inch long HE pellets slip fit
    wall tolerance 1 mil
    gives 1 % uncertainty in wall mass
- Scaled tests (consistency check)
  0.5 and 2 inch diameter HE
- Steady state flow
  Curved detonation front
    Approximately isentropic behind front
  Ringing in the wall (copper material strength)
  Radial variation of pressure
- Data
  Axial detonation speed
  Wall velocity from multiple probes

return

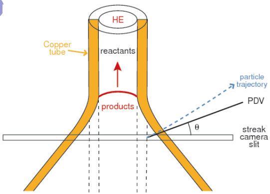

Log pressure

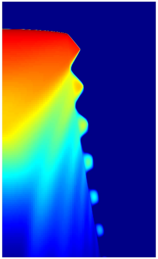

Cylinder test uncertainties

- Wall velocity variation
  With azimuthal angle
  wall thickness tolerance
- Detonation speed variation
  With lot and initial temperature
  Due to ρ_0 and curvature effect
- Wall expansion
  $R/R_0 \approx 3$ ($V/V_0 \approx 7$) at 15 μs
  $P \sim 0.1$ GPa
  Wall acceleration > 0 but decreasing
- Wall thins with expansion
  Thickness $\propto$ 1/Radius
  Spall at larger radii
- Fit products isentrope
  Match data with simulations

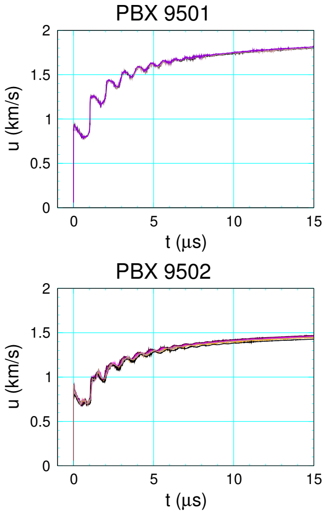

Pemberton *et al.*, 2011

CJ detonation speed

Experiments

- Planar detonation wave
  Thin flyer plate (short shock)
  Overdrive for prompt initiation
  Long enough run to decay to steady underdriven detonation
  Timing pins to measure detonation speed
- Extrapolate diameter effect
  $D(R) = D_{CJ}(1 - a/R)$ for large R
  Large diameter needed for PBX 9502 (X-0290)

0.5 to 2 inch ⇒ 7.70 km/s

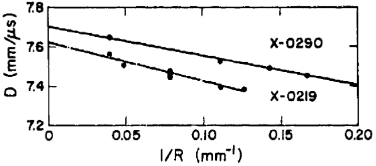

Campbell & Engelke 1976

2 and 4 inch ⇒ 7.78 km/s

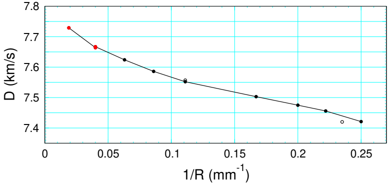

Campbell 1984

CJ pressure for CHE

Difficulty with applying shock jump conditions to CJ detonation
Unsupported detonation is followed by rarefaction
Difficult to tell where reaction zone ends and rarefaction begins VISAR profile

For CHE (thin reaction zone) Duff & Houston (1955)

1. Large diameter cylinder of HE initialized with plane wave lens
   Detonation front in neighborhood of axis is planar
2. Metal plate much thicker than reaction-zone width
   Shock match from reaction zone decays to match from CJ state
   Then decays at slower rate due to release rarefaction
3. Window and VISAR or PDV probes (at least 3 to measure tilt)
   Measure velocity at lead shock front
   From EOS of window and plate back out shock pressure
4. Series of experiments varying thickness of plate
   Extrapolate to zero plate thickness to account for rarefaction

CJ pressure for IHE

Overdriven detonations are shock like

u_p constant behind reaction zone
At CJ state, $\mathrm{d}u_s/\mathrm{d}u_p = 0$

Detonation locus for PBX 9502

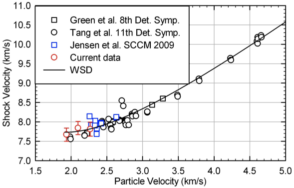

Gustavsen *et al.*, (2014), fig 4

- Fit locus in neighborhood of CJ
  $D = D_{cj} + a \cdot (u_p - u_{cj})^2$
  3 parameters: D_{cj}, u_{cj}, a
- Compare with D_{cj} from extrapolating diameter effect
  Estimate of uncertainty about 2 %
- Pressure from jump conditions
  $P_{cj} = \rho_0 u_{cj} D_{cj}$ (about 2 % uncertainty or $\pm$ 0.5 GPa)

If data too noisy use CJ release isentrope PDV or VISAR data
then assume Mie-Gruneisen form for local EOS
Fit to CJ isentrope and overdriven locus, see Wescott *et al.*, (2005) §IIB

Final remarks

- Accurate HE model for wide range of detonation phenomena
  Need a lot of calibration data, hence time and effort
- Correct for variation in initial density and temperature
  Need additional data
- When available data is incomplete
  Use estimates based on past experience with other HE
  Model is less accurate
- Predictive model, shock initiation and detonation propagation regimes
  Needed accuracy for application
    Design to avoid ignition thresholds
    Accident scenarios in more difficult regimes
  Model uncertainty
    Depends on accuracy of calibration data
    and meso-scale heterogeneities in HE
- Simulation accuracy
  Physical length scale (reaction-zone width) and resolution

Model calibration

- Select data to fit (subjective)
  Experiments aimed at single detonation phenomena
- Metric to compare model with multiple datasets (subjective)
  Simulated data for model (2-D simulation computationally expensive)
  Resolution for accurate simulation and uncertainty in data
- Calibration
  Iterative algorithm to vary parameters to minimize metric
- Issues
  Minimization is highly non-linear (local or global minimum)
  Metric may be insensitive to correlated changes in parameters
    or insufficient data may lead to underdetermined model
- Domain of applicability
  Tacit assumption: hotspot distribution same as calibration experiments
    Model accurate for applications similar to calibration experiments
    May loss accuracy for other applications

Detonation Waves in High Explosives

End of HE lecture series

Zoomed figures I

Detonation loci
Computer Micro-Tomography
VISAR profiles
PDV profiles
PBX 9501 micrograph
Proggram burn $D > D_{cj}$
Proggram burn $D < D_{cj}$
Wave diagram
Partly burned detonation loci
PBX 9501 V–P trajectory
PBX 9501 pressure profile
PBX 9501 compare resolution
Shock initiation – wedge experiment
Shock initiation – embedded gauges

Zoomed figures II

Zoomed figures III

Shock Polar
1D interaction
Oblique shock
2D wave pattern
Phermex shot 1037
Dn/Dz
Boundary layer y and kappa
Boundary layer pressure
Sonic locus
PBX 9501 wall velocity
PBX 9502 wall velocity
PBX 9502 detonation locus

Shock and Detonation loci

click to return

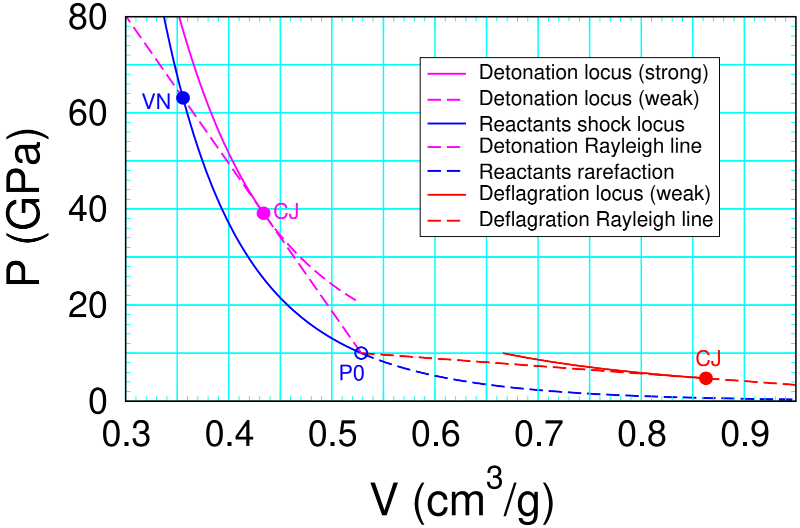

Micro-tomography image

click to return

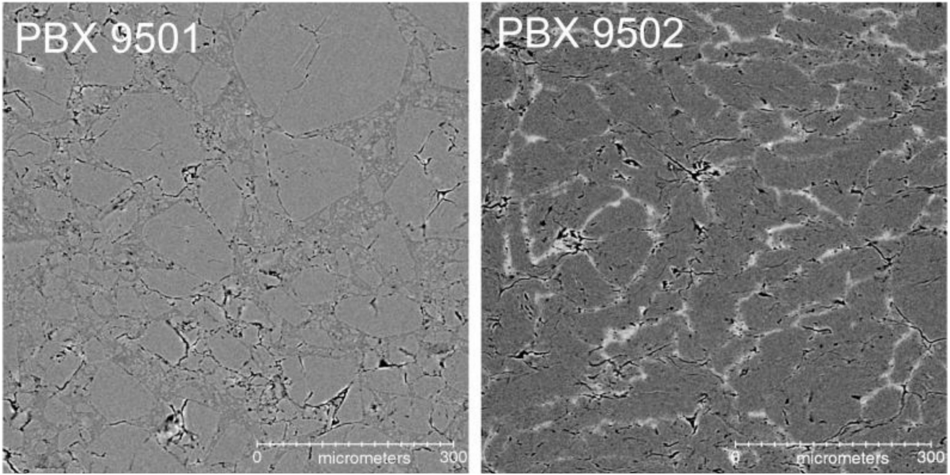

VISAR profile

PMMA window

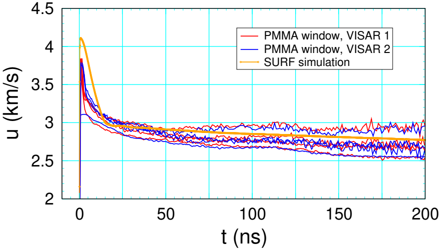

Li-F window

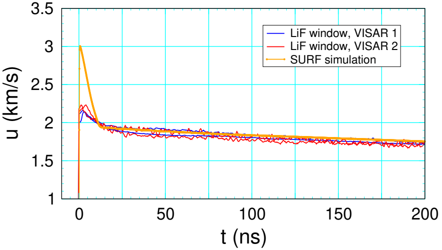

PDV profile

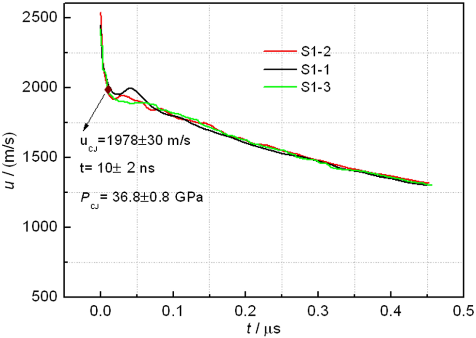

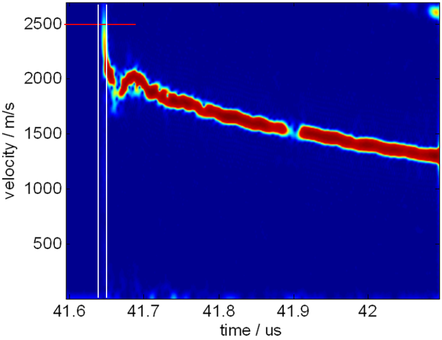

white guide lines
reaction time $\approx$ 10 ns

PBX 9501 polarized light micrograph

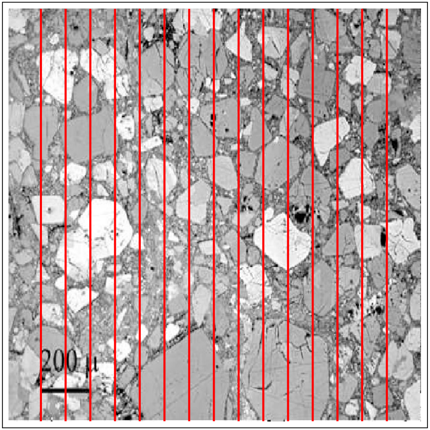

Red guide lines 100μm apart
Estimated reaction-zone width
based on curvature effect

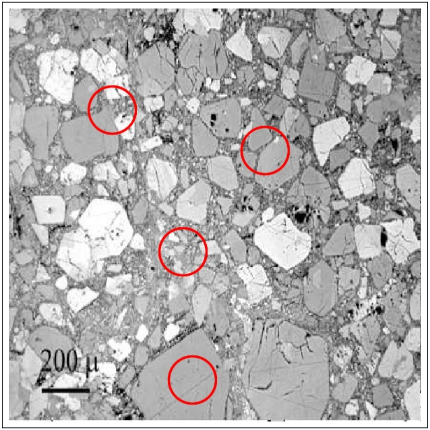

Red circles 200 μm diameter
VISAR or PDV spot size

Programmed burn $D > D_{cj}$

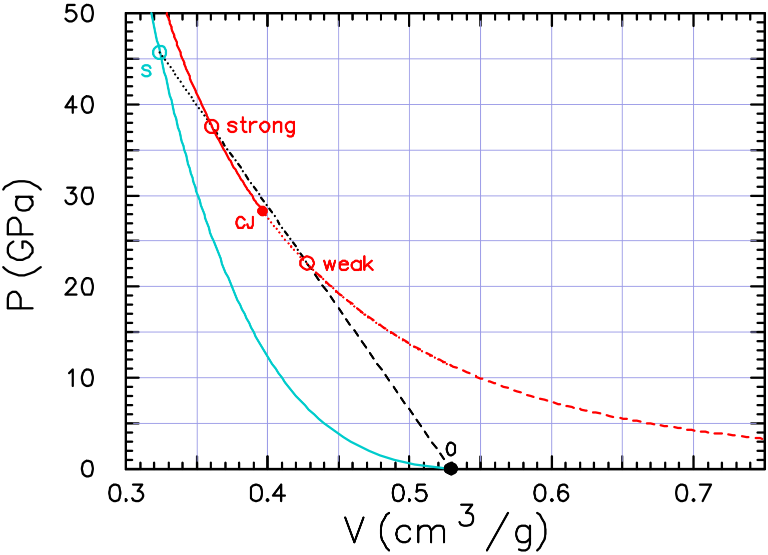

Programmed burn $D < D_{cj}$

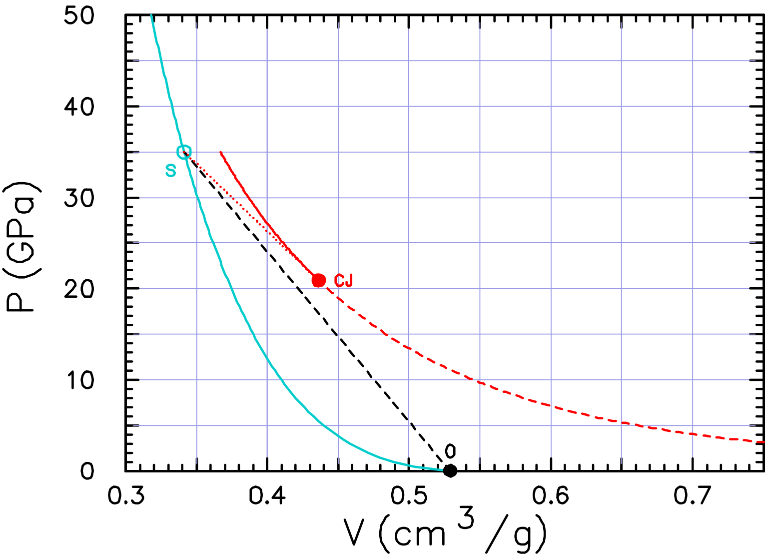

WaveDiagram

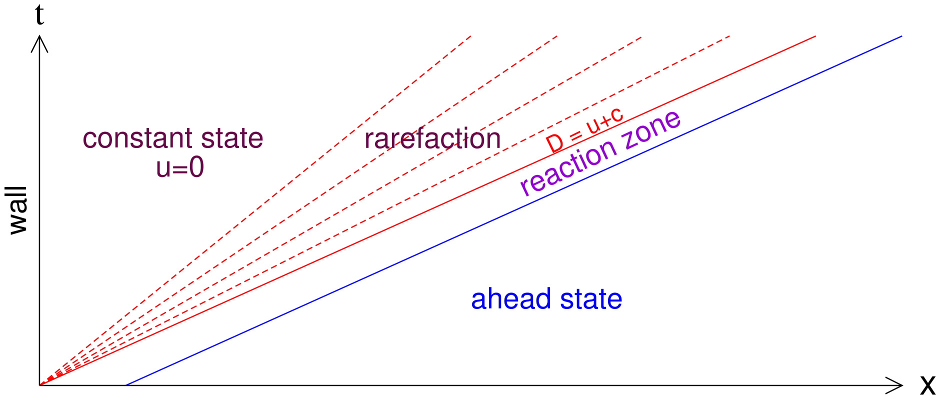

Partly burned detonation loci

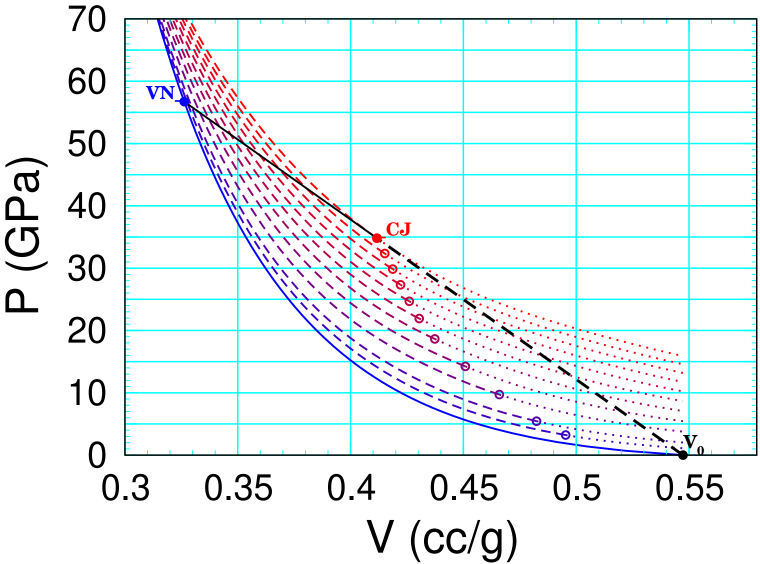

PBX 9501 V–P trajectory

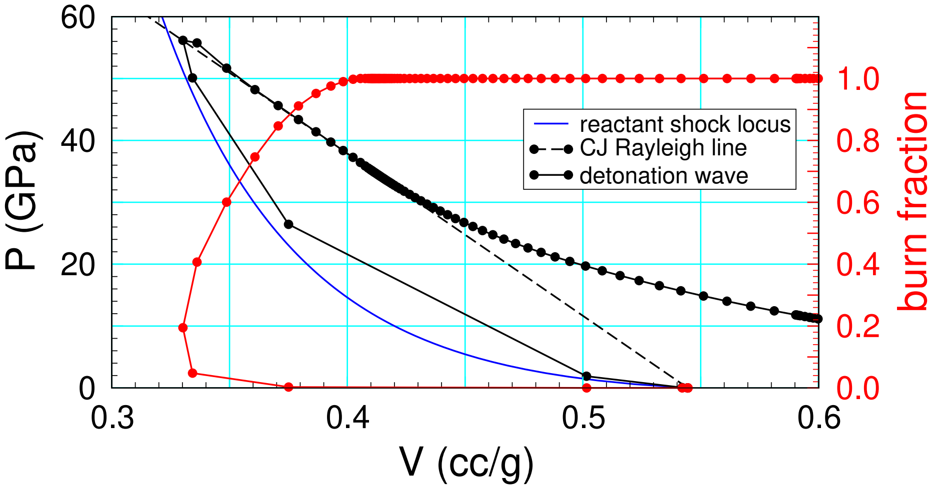

PBX 9501 pressure profile

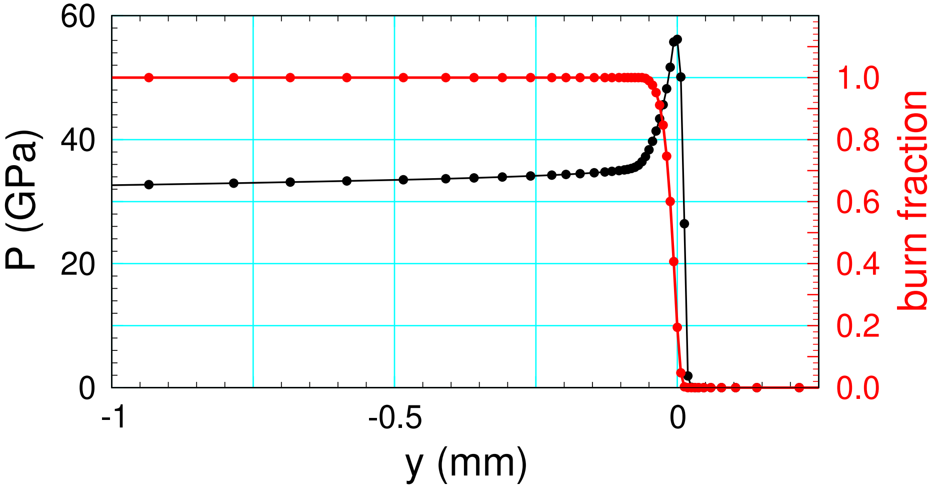

PBX 9501 compare resolution

Model reaction-zone width ≈ 70 microns

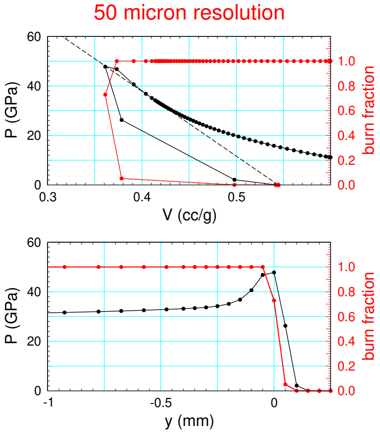

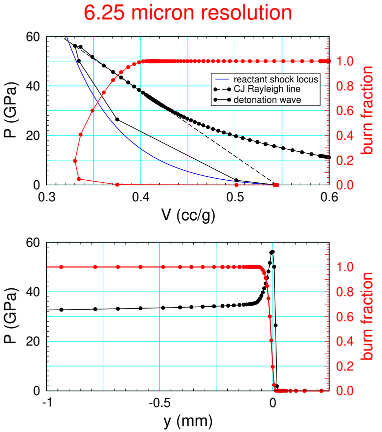

Effect of resolution is model and code dependent

This example is for SURF model in xRage code return

Shock initiation – wedge experiment

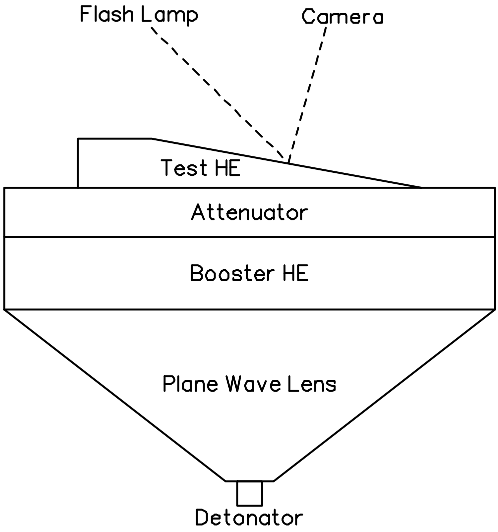

Shock initiation – embedded gauges

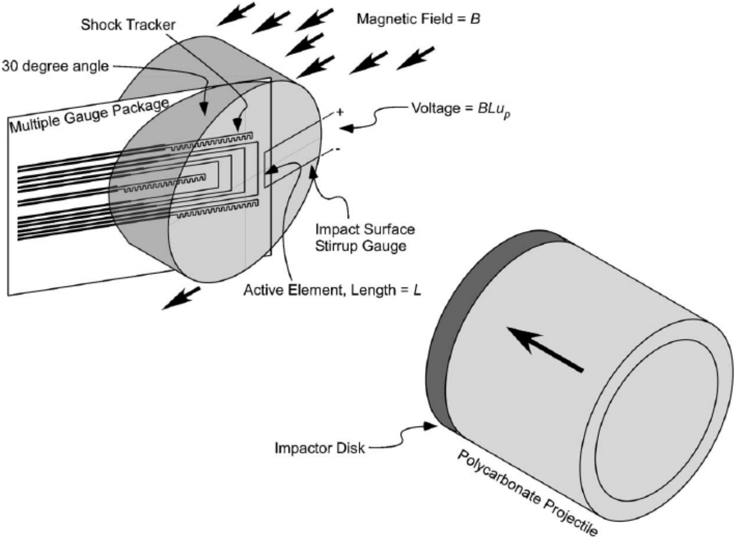

Pop plot data – shock trajectory

shock trajectory

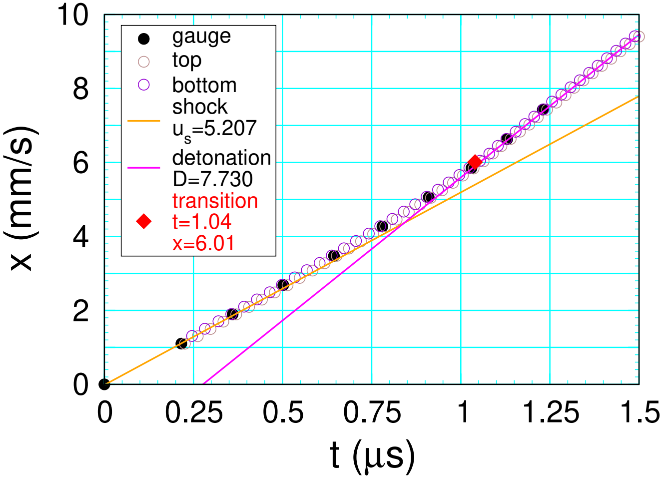

Pop plot data – velocity profiles

velocity profiles

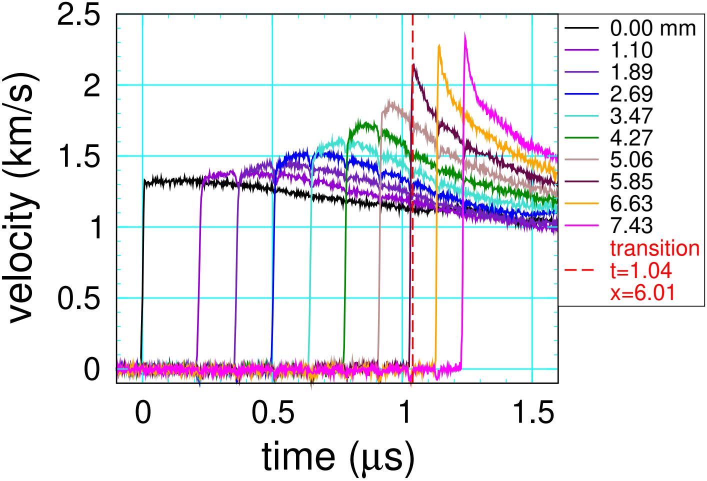

Pop plot – run distance

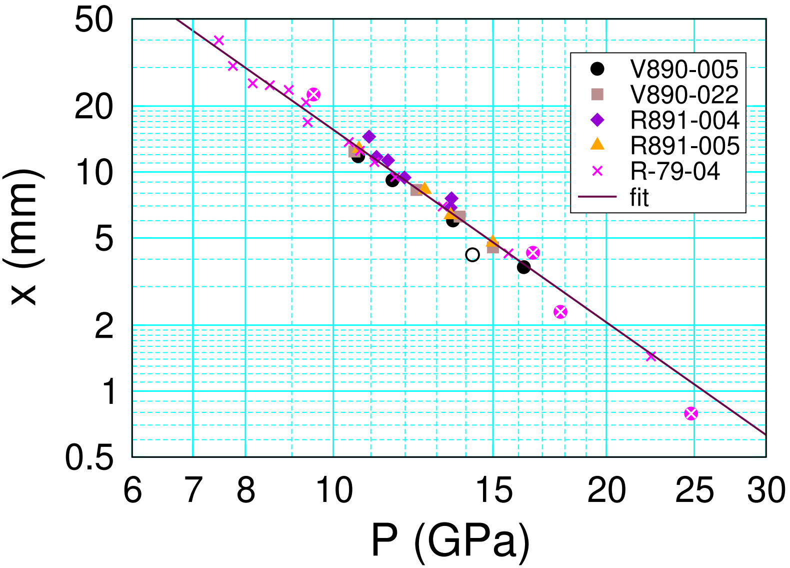

Pop plot – time to detonation

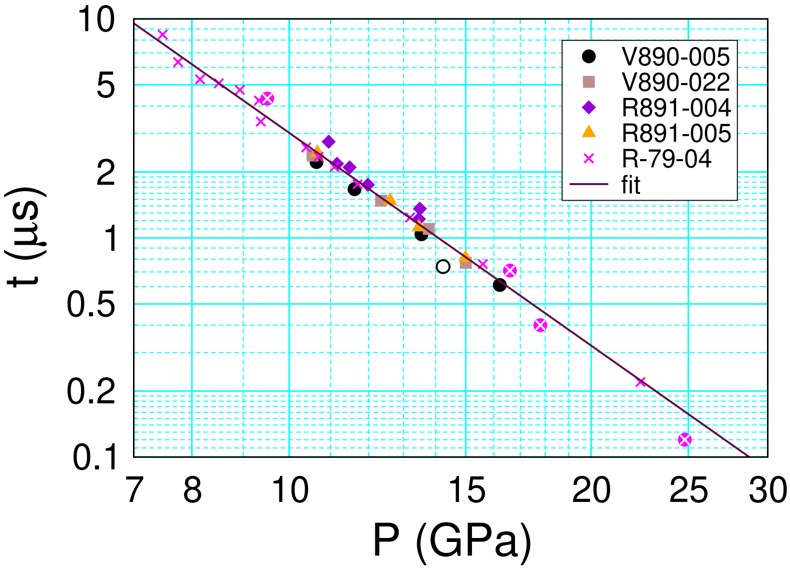

Pop plot – x(t)

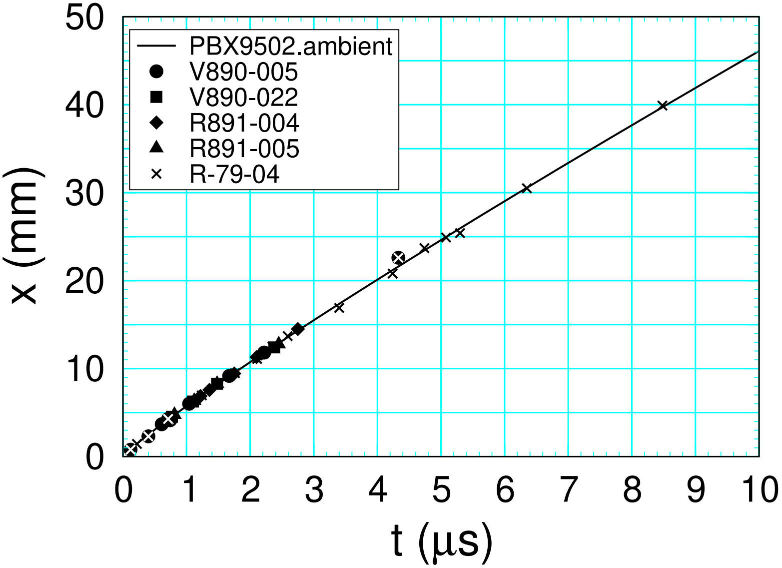
PBX9502.ambient
V890-005
V890-022
R891-004
R891-005
R-79-04
x (mm)
t (µs)
0
10
20
30
40
50
0
1
2
3
4
5
6
7
8
9
10

HMX Pop plot

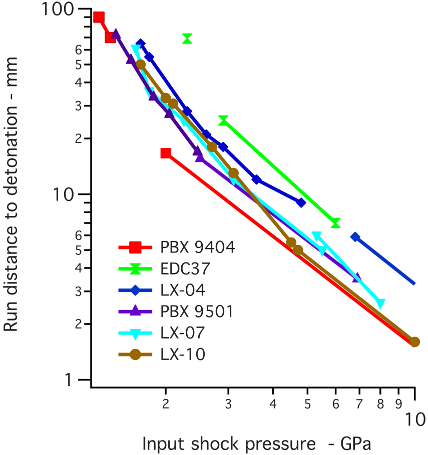

Vandersall *et al.*, 2010, fig 15 return

Pop plot x(P,T)

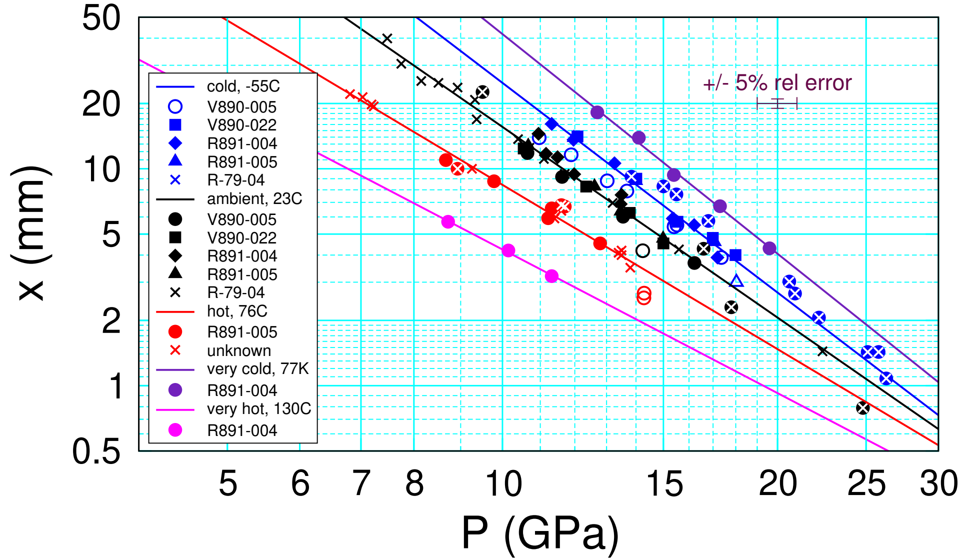

50
20
10
5
2
1
0.5
x (mm)
5
6
7
8
10
15
20
25
30
P (GPa)
cold, -55C
V890-005
V890-022
R891-004
R891-005
R-79-04
ambient, 23C
V890-005
V890-022
R891-004
R891-005
R-79-04
hot, 76C
R891-005
unknown
very cold, 77K
R891-004
very hot, 130C
R891-004
+/- 5% rel error

Pop plot t(P,T)

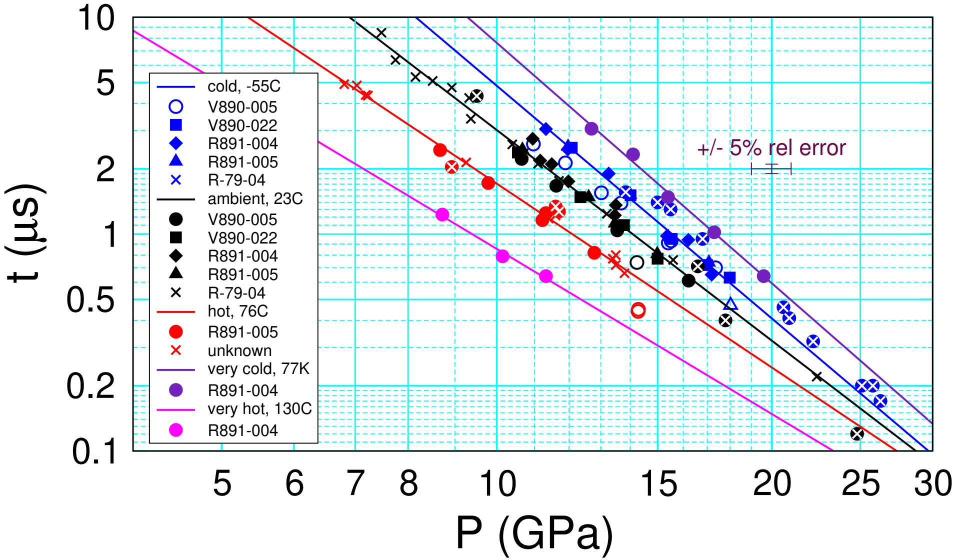

10
5
2
1
0.5
0.2
0.1
t (µs)
5
6
7
8
10
15
20
25
30
P (GPa)
cold, -55C
V890-005
V890-022
R891-004
R891-005
R-79-04
ambient, 23C
V890-005
V890-022
R891-004
R891-005
R-79-04
hot, 76C
R891-005
unknown
very cold, 77K
R891-004
very hot, 130C
R891-004
+/- 5% rel error

Match hotspot at CJ state → reactants

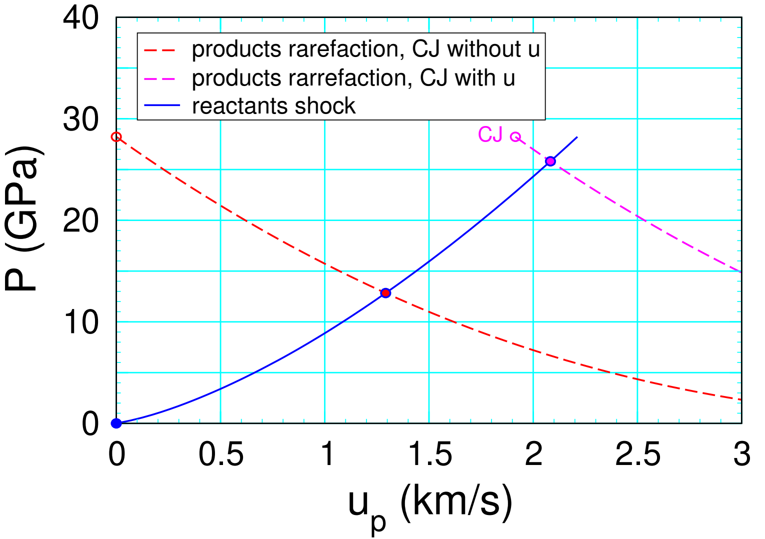

PBX 9501 – global rate (Henson & Smilowitz)

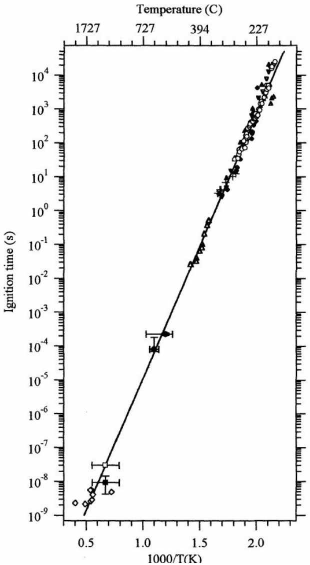

Diameter effect: D vs 1/R

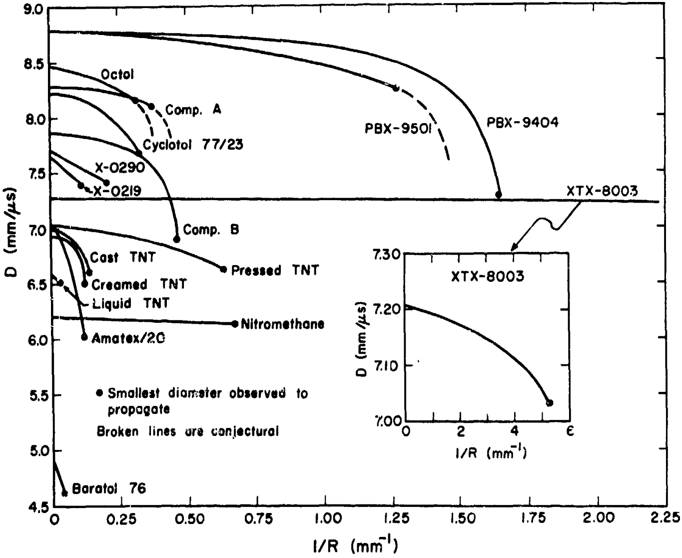

Profile ODEs with curvature

Quasi-steady profile ODEs with front curvature κ ◂ return

$$-\left[c^2 - (D-u)^2\right] \frac{\mathrm{d}}{\mathrm{d}x} \begin{pmatrix} V \\ D-u \\ \lambda \end{pmatrix} = \begin{pmatrix} \left[\sigma\,\mathcal{R}\,c^2 - u\,\kappa\,(D-u)^2\right] V/(D-u) \\ (\sigma\mathcal{R} - u\,\kappa)\,c^2 \\ \left[c^2 - (D-u)^2\right]\mathcal{R}/(D-u) \end{pmatrix}$$

plus Bernoulli equation $e + P\,V + \frac{1}{2}(D-u)^2 = \text{constant}$
where $\sigma = (\partial_\lambda P)_{V,e}/(\rho c^2)$ is thermicity

$$\kappa \begin{cases} > 0, & \text{diverging front, unsupported detonation} \\ = 0, & \text{planar front, reduces to ZND profile} \\ < 0, & \text{converging front, overdriven detonation} \end{cases}$$

- Diverging detonation wave
  $D_n(\kappa)$ determined by "eigenvalue" like problem
  ODE trajectory with $\sigma\mathcal{R} - u\kappa = 0$ at critical point $[c^2 - (D-u)^2] = 0$
- Sonic point within reaction zone
  D_n decreases as κ increases

Resolution and curvature effect

Axial detonation speed for cylinder test

Examples of dependence on numerical resolution

Cell size from 6.25 to 200 microns

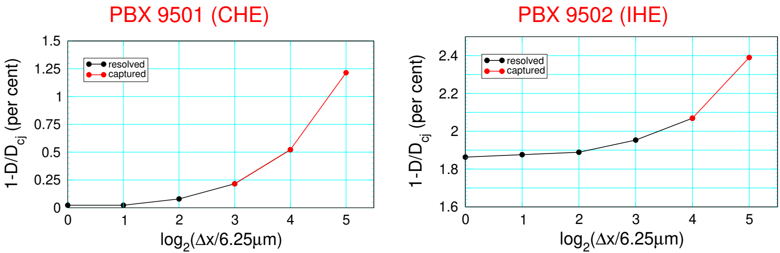

Accuracy decreases rapidly when reaction zone captured

i.e., cell size $\gtrsim$ reaction-zone width

Convergence rate is model and code dependent

These examples are for SURF model in xRage code, Menikoff, 2019

return

PBX 9502 profile

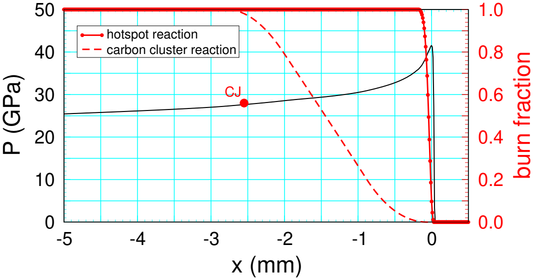

return

Shock polar

◂ return

1-D shock interaction
P and u continuous
across contact
particle trajectory $\sim$ time direction

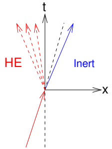

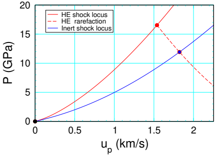

Oblique shock
& turning angle

$$\tan\theta = \frac{u_p u_s}{q_0^2 - u_p u_s} \cdot \frac{q_\parallel}{u_s}$$

$$q_\parallel^2 = q_0^2 - u_s^2$$

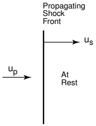

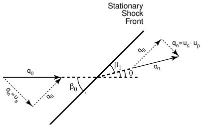

Steady 2-D wave pattern
P and $u_\perp$ continuous
$u_\parallel$ discontinuous (slip line)
across contact
streamline $\parallel$ contact
streamline $\sim$ time direction

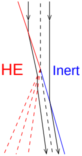

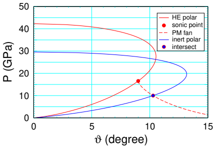

1-D interaction

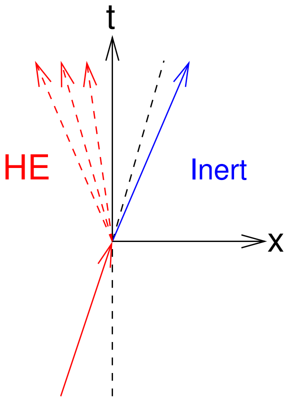

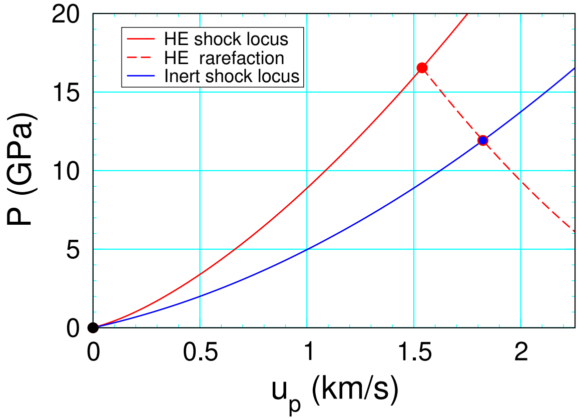

Oblique shock

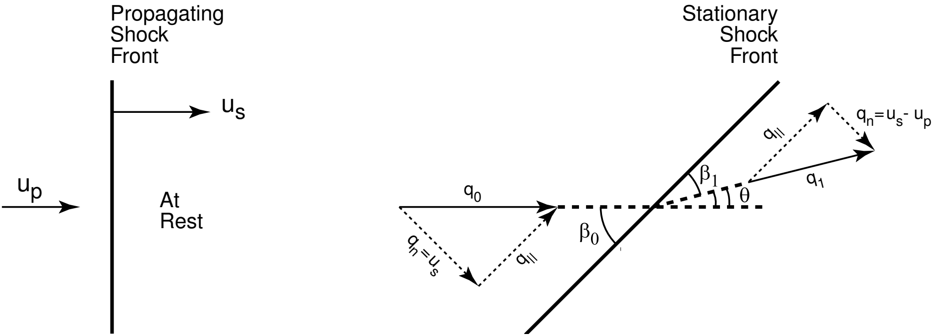

2-D wave pattern

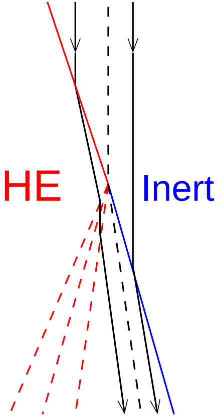

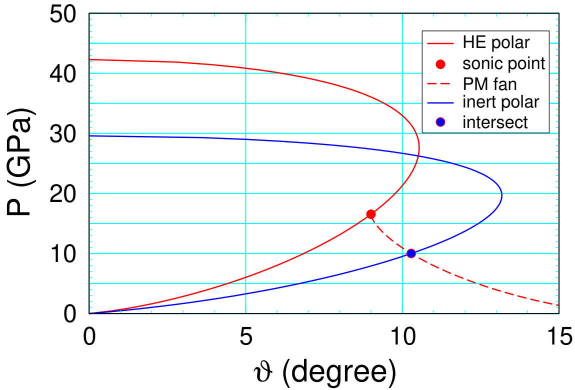

Intersecting detonation wave fronts

return

Phermex shot 1037

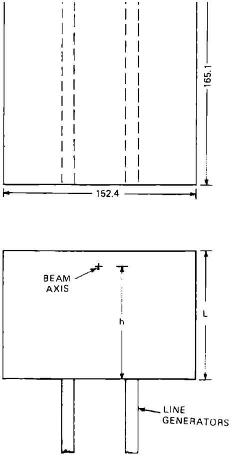

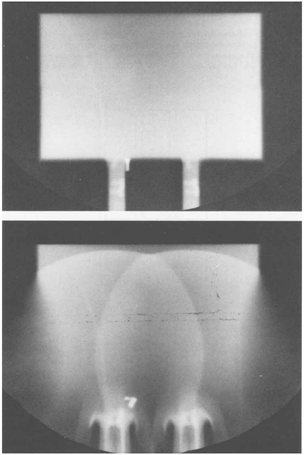

Experimental measurement of $D_n(\kappa)$

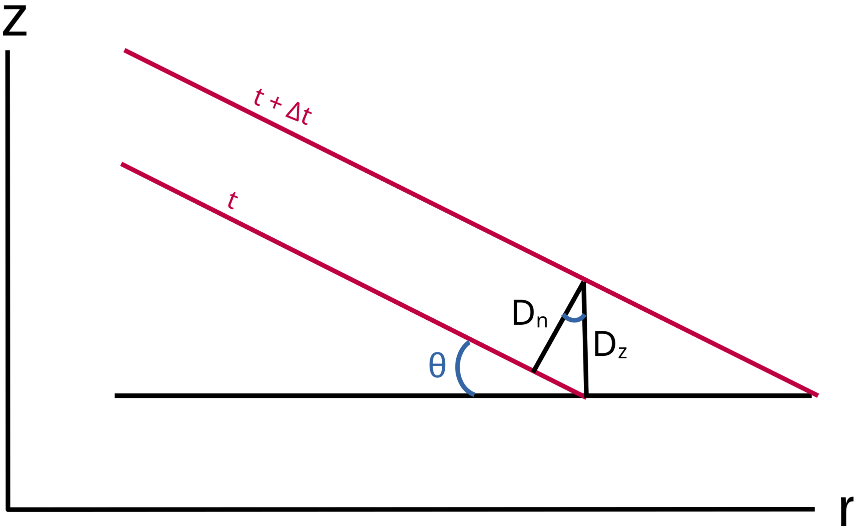

Boundary layer y and κ

normalized front shape

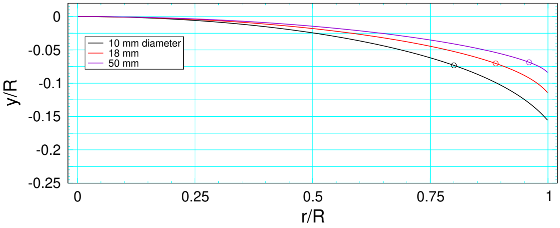

curvature vs normalized radius

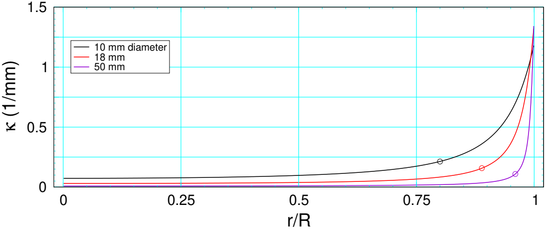

Boundary layer pressure

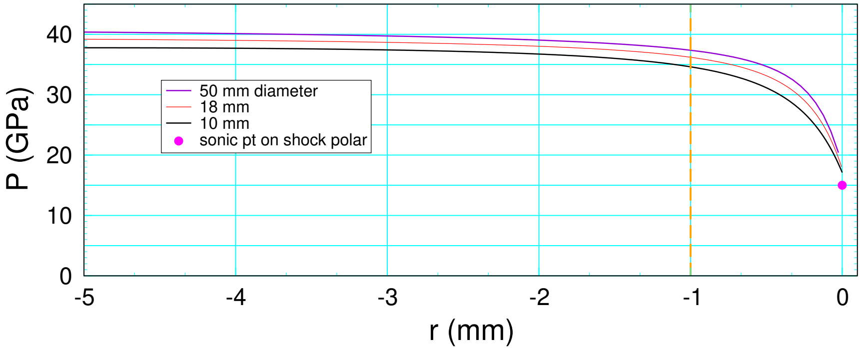

Sonic locus

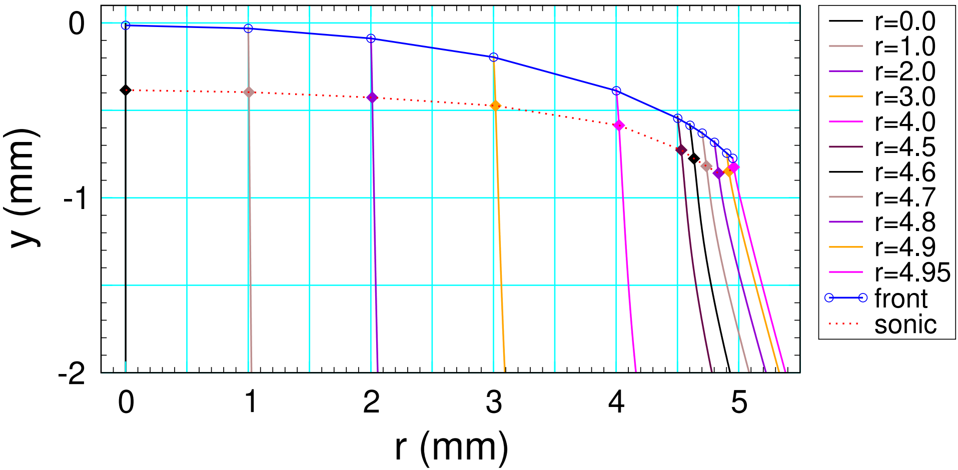
0
-1
-2
y (mm)
0
1
2
3
4
5
r (mm)
r=0.0
r=1.0
r=2.0
r=3.0
r=4.0
r=4.5
r=4.6
r=4.7
r=4.8
r=4.9
r=4.95
front
sonic

PBX 9501 wall velocity

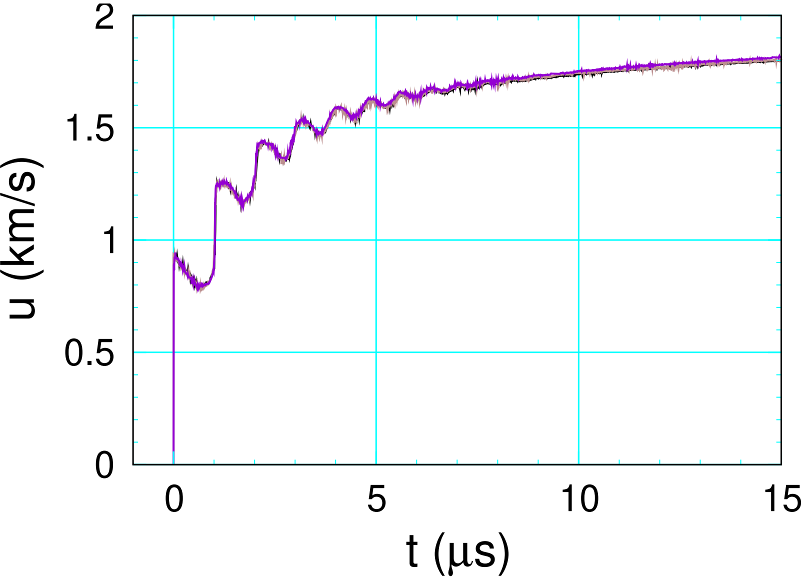

PBX 9502 wall velocity

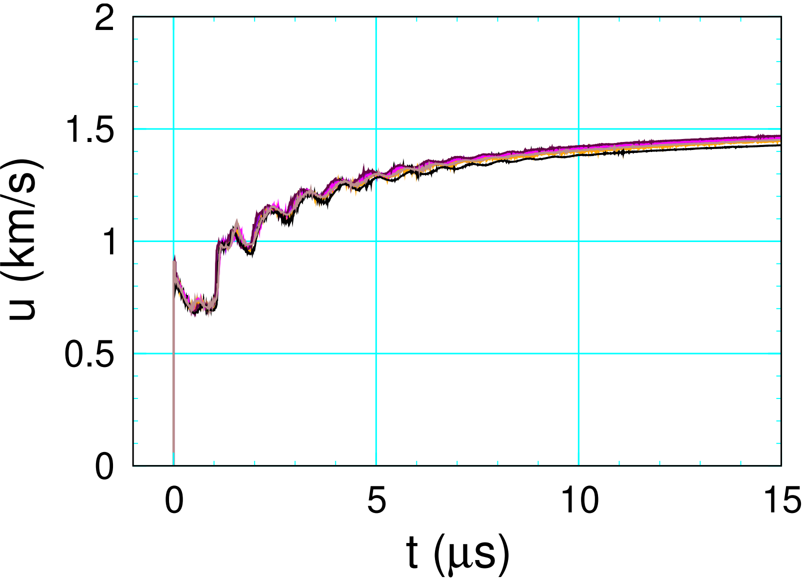

PBX 9502 detonation locus